termined whether this promoted insulin resistance when injected into mice. Intraperitoneal injection of insulin (0.5 U/kg) and purified Klotho extracellular peptide (10 μg/kg, Fig. 2F) in wild-type male and female mice attenuated the hypoglycemic response expected from insulin alone (Fig. 2G). Klotho peptide alone rapidly increased blood glucose levels in male wild-type mice and to a smaller extent in females (Fig. 2H). However, Klotho peptide injection did not induce significant changes in blood insulin and glucagon levels (fig. S4), suggesting that Klotho peptide inhibits insulin action directly in peripheral tissues.

To test whether Klotho antagonizes insulin at receptive cells, we determined whether recombinant Klotho peptide would reduce glucose uptake by blocking insulin binding to the insulin receptor. We measured cellular glucose uptake in cultured myoblastic cells (L6) incubated with or without insulin in the presence or absence of 100 pM of Klotho extracellular peptide. Klotho peptide suppressed insulin-induced glucose uptake by 55% without reducing the binding of [^{125}I] insulin to the cells (fig. S5). Thus, Klotho does not appear to inhibit ligand-binding to the insulin receptor, suggesting that Klotho may block insulin action by disrupting one or more alternative insulin-dependent intracellular signaling pathways. Accordingly, we measured the potential for [^{125}I]-labeled Klotho to bind directly to the cell surface. Hepatoma cells bound [^{125}I] Klotho in a dose-dependent manner and saturated when the total Klotho concentration exceeded 600 pM, and unlabeled Klotho peptide inhibited the binding of [^{125}I] Klotho (fig. S6). Together, these observations suggest that cells present a receptor at their surface other than the insulin receptor that binds to the Klotho peptide.

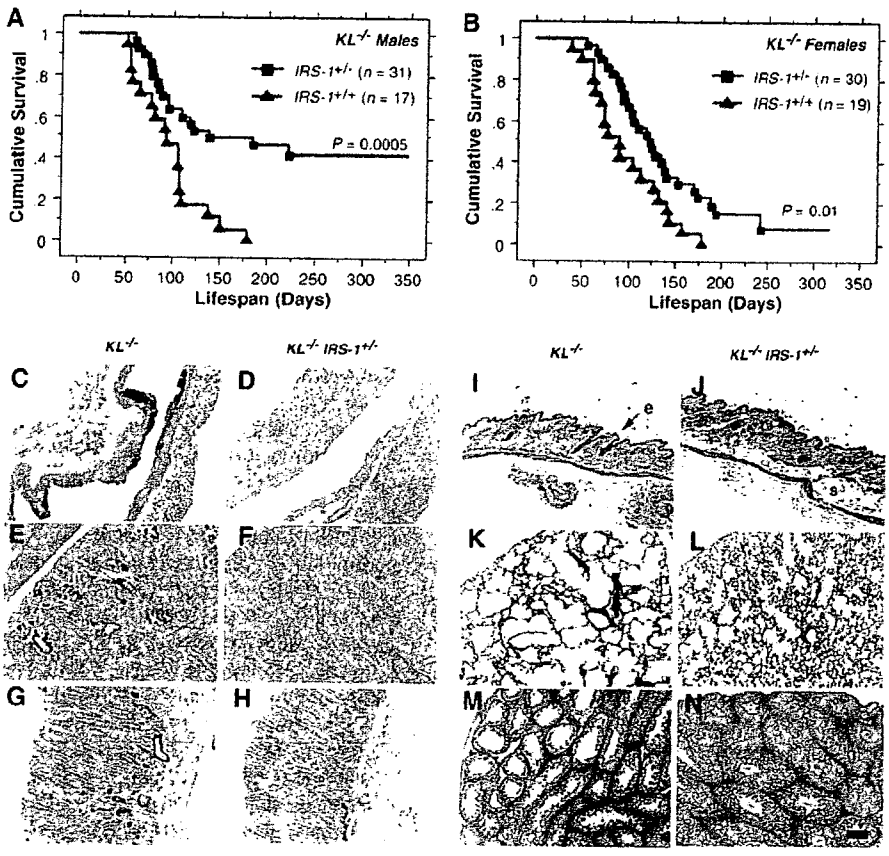

Fig. 4. Rescue of aging-like phenotypes in $KL^{-/-}$ mice by genetic intervention in insulin and IGF1 signaling. (A and B) Life-span extension in $KL^{-/-}$ mice by reducing IRS-1 expression. $KL^{-/-}$ mice heterozygous for an IRS-1 null allele ($IRS\text{-}1^{+/-}$) lived longer than those without the mutation ($IRS\text{-}1^{+/+}$) both in males ($P = 0.0005$ by log-rank test) and females ($P = 0.01$ by log-rank test). [(C) to (N)] Rescue of aging-like phenotypes in $KL^{-/-}$ $IRS\text{-}1^{+/-}$ mice at the histological level. Typical findings from four 8-week-old males of each genotype are shown. (C and D) Aorta (von Kossa staining). Calcification of arterial walls [black deposits in (C)] was decreased in $KL^{-/-}$ $IRS\text{-}1^{+/-}$ mice (D). (E and F) Kidney (von Kossa staining). Calcification of small arteries and renal tubules [black deposits in (E)] was decreased in $KL^{-/-}$ $IRS\text{-}1^{+/-}$ mice (F). (G and H) Stomach (von Kossa staining). Ectopic calcification in gastric mucosa and small arteries [black deposits in (G)] was alleviated in $KL^{-/-}$ $IRS\text{-}1^{+/-}$ mice (H). (I and J) Cross-sections of the skin. Hematoxylin-eosin (HE) staining. Reduction in epidermal layer (e) thickness observed in $KL^{-/-}$ mice (I) was improved and subcutaneous fat (s) was restored in $KL^{-/-}$ $IRS\text{-}1^{+/-}$ mice (J). (K and L) Lung (HE staining). Emphysematous changes, including enlargement of air spaces and destruction of the normal alveolar architecture were observed in $KL^{-/-}$ mice (K), but were alleviated in $KL^{-/-}$ $IRS\text{-}1^{+/-}$ mice (L). (M and N) Testis (HE staining). Seminiferous tubules were atrophic and no mature sperm was observed in $KL^{-/-}$ mice (M). Spermatogenesis was restored in $KL^{-/-}$ $IRS\text{-}1^{+/-}$ mice (N). All panels were shown in the identical magnification (×200). Scale bar, 200 μm.

Klotho inhibits intracellular insulin and IGF1 signaling. Because membrane-bound Klotho peptide must inhibit ligand activation of the insulin receptor within the cells, we investigated the influence of Klotho on insulin receptor signal transduction (*25*, *26*). We incubated L6 cells or rat hepatoma cells (H4IIE) with recombinant Klotho peptide and insulin (10 nM) or IGF1 (10 nM). Klotho peptide did not inhibit the binding of [^{125}I] insulin or [^{125}I] IGF1 (fig. S5) but suppressed ligand-stimulated autophosphorylation of insulin and IGF1 receptors in a dose-dependent manner (Fig. 3, A and B). Additionally, Klotho reduced activation of signaling events downstream of receptor activation, including tyrosine-phosphorylated insulin receptor substrate (IRS) 1 and 2, the association of the subunit of phosphoinositide 3-kinase p85 with IRS proteins (Fig. 3, A and B). Because the inhibitory effect of Klotho on insulin signaling was observed as early as 1 min after insulin stimulation (Fig. 3C), the decline in tyrosine-phosphorylated insulin and IGF1 receptors is unlikely due simply to the loss of receptors. Notably, Klotho peptide can inactivate active insulin receptors that were previously tyrosine phosphorylated by insulin stimulation. In H4IIE cells that were exposed to 10 nM insulin before adding Klotho peptide, Klotho suppressed tyrosine phosphorylation of the insulin receptor (Fig. 3D). We observed a similar effect on IGF1 receptor autophosphorylation in L6 cells with IGF1 before adding Klotho peptide (*9*). Importantly, the inhibitory effect of Klotho on autophosphorylation of receptor tyrosine kinases is specific. We observed no inhibitory effect of Klotho on the epidermal growth factor receptor and the platelet-derived growth factor receptor (fig. S7). Overall, Klotho appears to inhibit activation of the insulin and IGF1 receptor and to repress activated insulin and IGF1 receptors. Whether Klotho peptide functions by accelerating removal of tyrosine phosphorylation from the activated insulin receptor remains to be determined.

Inhibition of insulin and IGF1 signaling rescues $KL^{-/-}$ phenotypes. If the ability of Klotho to inhibit insulin and IGF1 signaling extends survival by retarding senescence, independent manipulations to inhibit insulin and IGF1 signaling may ameliorate some of the aging-like phenotypes in $KL^{-/-}$ mice. Accordingly, we crossed a loss-of-function mutation of IRS-1 into the $KL^{-/-}$ mice (*27*). Survival was improved in $KL^{-/-}$ mice heterozygous for an IRS-1 null allele ($KL^{-/-}$ $IRS\text{-}1^{+/-}$) relative to $KL^{-/-}$ control mice

(Fig. 4, A and B). In addition, $KL^{-/-}$ *IRS-1*$^{+/-}$ mice ameliorated many age-related pathologies typical of $KL^{-/-}$ mice, including arteriosclerosis, ectopic calcification, skin atrophy, pulmonary emphysema, and hypogonadism (Fig. 4, C to N). Heterozygosity of IRS-1 alone ($KL^{+/+}$ *IRS-1*$^{+/-}$ littermates) appears to have no effect on survival and the age-progressive degeneration when compared with those factors in wild-type littermates during these experiments (*9*).

Conclusion. We previously reported that a defect in *Klotho* gene expression leads to a syndrome that may resemble premature aging (*1*). Here, we show that overexpression of *Klotho* can extend life span, and we suggest that *Klotho* functions as an aging suppressor gene in mammals. We found that the extracellular domain of Klotho protein circulates in the blood and binds to a putative cell-surface receptor. Klotho has marked effects on insulin physiology, apparently because it suppresses tyrosine phosphorylation of insulin and IGF1 receptors, which results in reduced activity of IRS proteins and their association with PI3-kinase, thereby inhibiting insulin and IGF1 signaling. Extended life span upon negative regulation of insulin and IGF1 signaling is an evolutionarily conserved mechanism to suppress aging (*28*). Klotho appears to be a peptide hormone to modulate such signaling and thereby mediate insulin metabolism and aging.

References and Notes

1. M. Kuro-o *et al.*, *Nature* 390, 45 (1997).
2. Y. Takahashi, M. Kuro-o, F. Ishikawa, *Proc. Natl. Acad. Sci. U.S.A.* 97, 12407 (2000).
3. D. E. Arking *et al.*, *Proc. Natl. Acad. Sci. U.S.A.* 99, 856 (2002).
4. D. E. Arking *et al.*, *Am. J. Hum. Genet.* 72, 1154 (2003).
5. N. Ogata *et al.*, *Bone* 31, 37 (2002).
6. K. Kawano *et al.*, *J. Bone Miner. Res.* 17, 1744 (2002).
7. Y. Yamada, F. Ando, N. Niino, H. Shimokata, *J. Mol. Med.* 83, 50 (2005).
8. D. E. Arking, G. Atzmon, A. Arking, N. Barzilai, H. C. Dietz, *Circ. Res.* 96, 412 (2005).
9. M. Kuro-o *et al.*, data not shown.
10. F. Grabnitz, M. Seiss, K. P. Rucknagel, W. L. Staudenbauer, *Eur. J. Biochem.* 200, 301 (1991).
11. R. Weindruch, R. L. Walford, S. Fligiel, D. Guthrie, *J. Nutr.* 116, 641 (1986).
12. H. M. Brown-Borg, K. E. Borg, C. J. Meliska, A. Bartke, *Nature* 384, 33 (1996).
13. R. A. Miller, *Sci. Aging Knowledge Environ.* 2001, vp6 (2001).
14. G. C. Williams, *Evol. Int. J. Org. Evol.* 11, 398 (1957).
15. C. Kenyon, J. Chang, E. Gensch, A. Rudner, R. Tabtiang, *Nature* 366, 461 (1993).
16. J. Z. Morris, H. A. Tissenbaum, G. Ruvkun, *Nature* 382, 536 (1996).
17. M. Tatar *et al.*, *Science* 292, 107 (2001).
18. D. J. Clancy *et al.*, *Science* 292, 104 (2001).
19. M. Holzenberger *et al.*, *Nature* 421, 182 (2003).
20. M. Bluher, B. B. Kahn, C. R. Kahn, *Science* 299, 572 (2003).
21. C. Kenyon, *Cell* 120, 449 (2005).
22. T. Utsugi *et al.*, *Metabolism* 49, 1118 (2000).
23. A. E. Halseth, D. P. Bracy, D. H. Wasserman, *Am. J. Physiol.* 276, E70 (1999).
24. A. Imura *et al.*, *FEBS Lett.* 565, 143 (2004).
25. A. R. Saltiel, C. R. Kahn, *Nature* 414, 799 (2001).
26. D. LeRoith, C. T. Roberts Jr., *Cancer Lett.* 195, 127 (2003).
27. E. Araki *et al.*, *Nature* 372, 186 (1994).
28. M. Tatar, A. Bartke, A. Antebi, *Science* 299, 1346 (2003).

29. We thank D. H. Wasserman and Vanderbilt Mouse Metabolic Phenotyping Center for physiological analysis of the mice; R. L. Dobbins for hyperinsulinemic euglycemic clamp experiments; J. A. Richardson and Molecular Pathology Core Facility at UT Southwestern for histological analysis; D. W. Russell at UT Southwestern for Klotho receptor identification; R. Komuro and H. Kuriyama at UT Southwestern for insulin and IGF1 signaling analysis; Genentech for providing IGF1; H. Masuda, T. Suga, R. Nagai, A. T. Dang, R. Shamlou, P. Bezzera, T. Reed, C. Iucu, W. Lai for earlier contributions and supports to this study; and E. C. Friedberg, M. S. Brown, and K. A. Wharton Jr. at UT Southwestern for critical reading of the manuscript. This work was supported in part by grants from Endowed Scholar Program at UT Southwestern (M.K.), Pew Scholars Program in Biomedical Science (M.K.), Eisai Research Fund (M.K.), High-Impact/High-Risk Research Program at UT Southwestern (M.K.), and NIH (R01AG19712 to M.K. and R01AG25326 to M.K. and K.P.R.). J.H. is supported by the NIH, the Perot Family Foundation, and the Humboldt Foundation.

Supporting Online Material
www.sciencemag.org/cgi/content/full/1112766/DC1
Materials and Methods
Figs. S1 to S7
Table S1
References

25 March 2005; accepted 4 August 2005
Published online 25 August 2005;
10.1126/science.1112766
Include this information when citing this paper.

REPORTS

Bright X-ray Flares in Gamma-Ray Burst Afterglows

D. N. Burrows,[1]* P. Romano,[2] A. Falcone,[1] S. Kobayashi,[1,3] B. Zhang,[4] A. Moretti,[2] P. T. O'Brien,[5] M. R. Goad,[5] S. Campana,[2] K. L. Page,[5] L. Angelini,[6,7] S. Barthelmy,[6] A. P. Beardmore,[5] M. Capalbi,[8] G. Chincarini,[2,9] J. Cummings,[6] G. Cusumano,[10] D. Fox,[11] P. Giommi,[8] J. E. Hill,[1] J. A. Kennea,[1] H. Krimm,[6] V. Mangano,[10] F. Marshall,[6] P. Mészáros,[1] D. C. Morris,[1] J. A. Nousek,[1] J. P. Osborne,[5] C. Pagani,[1,2] M. Perri,[8] G. Tagliaferri,[2] A. A. Wells,[5] S. Woosley,[12] N. Gehrels[6]

Gamma-ray burst (GRB) afterglows have provided important clues to the nature of these massive explosive events, providing direct information on the nearby environment and indirect information on the central engine that powers the burst. We report the discovery of two bright x-ray flares in GRB afterglows, including a giant flare comparable in total energy to the burst itself, each peaking minutes after the burst. These strong, rapid x-ray flares imply that the central engines of the bursts have long periods of activity, with strong internal shocks continuing for hundreds of seconds after the gamma-ray emission has ended.

Gamma-ray bursts (GRBs) are the most powerful explosions since the Big Bang, with typical energies around 10^{51} ergs. Long GRBs (duration > 2 s) are thought to signal the creation of black holes by the collapse of massive stars (*1–4*). The detected signals from the resulting highly relativistic fireballs consist of prompt gamma-ray emission (from internal shocks in the fireball) lasting for several seconds to minutes, followed by afterglow emission (from external shocks as the fireball encounters surrounding material) covering a broad range of frequencies from radio through x-rays (*5–7*). Because of the time needed to accurately determine the GRB position, most afterglow

[1]Department of Astronomy and Astrophysics, 525 Davey Lab, Pennsylvania State University, University Park, PA 16802, USA. [2]Istituto Nazionale di Astrofisica (INAF)–Osservatorio Astronomico di Brera, Via Bianchi 46, 23807 Merate, Italy. [3]Center for Gravitational Wave Physics, 104 Davey Lab, Pennsylvania State University, University Park, PA 16802, USA. [4]Department of Physics, University of Nevada, Box 454002, Las Vegas, NV 89154–4002, USA. [5]Department of Physics and Astronomy, University of Leicester, University Road, Leicester LE1 7RH, UK. [6]NASA/Goddard Space Flight Center, Greenbelt, MD 20771, USA. [7]Department of Physics and Astronomy, Johns Hopkins University, 3400 North Charles Street, Baltimore, MD 21218, USA. [8]Agenzia Spaziale Italiana Science Data Center, Via Galileo Galilei, 00044 Frascati, Italy. [9]Dipartimento di Fisica, Università degli studi di Milano-Bicocca, Piazza delle Scienze 3, 20126 Milan, Italy. [10]INAF–Istituto di Astrofisica Spaziale e Fisica Cosmica Sezione di Palermo, Via Ugo La Malfa 153, 90146 Palermo, Italy. [11]Department of Astronomy, California Institute of Technology, MS 105-24, Pasadena, CA, 91125, USA. [12]Department of Astronomy and Astrophysics, University of California, Santa Cruz, CA 95064, USA.

*To whom correspondence should be addressed. E-mail: burrows@astro.psu.edu

THE JOURNAL OF BIOLOGICAL CHEMISTRY VOL. 280, NO. 42, pp. 35704–35712, October 21, 2005

Involvement of Endogenous Bone Morphogenetic Protein (BMP) 2 and BMP6 in Bone Formation*

Received for publication, May 11, 2005, and in revised form, August 17, 2005 Published, JBC Papers in Press, August 18, 2005, DOI 10.1074/jbc.M505166200

Fumitaka Kugimiya[‡§], Hiroshi Kawaguchi[§], Satoru Kamekura[§], Hirotaka Chikuda[§], Shinsuke Ohba[‡], Fumiko Yano[‡], Naoshi Ogata[‡], Takenobu Katagiri[¶], Yoshifumi Harada[‖], Yoshiaki Azuma[‖], Kozo Nakamura[§], and Ung-il Chung[‡1]

From the Divisions of [‡]Tissue Engineering and [§]Sensory & Motor System Medicine, Faculty of Medicine, University of Tokyo, Hongo 7-3-1, Bunkyo, Tokyo, 113-8655, the [¶]Division of Pathophysiology, Research Center for Genomic Medicine, Saitama Medical School, Yamane 1397-1, Hidaka, Saitama, 350-1241, and [‖]Teijin Co., Ltd., Asahigaoka 4-3-2, Hino, Tokyo 191-8512, Japan

Although accumulated evidence has shown the bone anabolic effects of bone morphogenetic proteins (BMPs) that were exogenously applied *in vitro* and *in vivo*, the roles of endogenous BMPs during bone formation remain to be clarified. This study initially investigated expression patterns of BMPs in the mouse long bone and found that BMP2 and BMP6 were the main subtypes expressed in hypertrophic chondrocytes that induce endochondral bone formation. We then examined the involvement of the combination of these BMPs in bone formation *in vivo* by generating the compound-deficient mice (*Bmp2*+/−;*Bmp6*−/−). Under physiological conditions, these mice exhibited moderate growth retardation compared with the wild-type (WT) littermates during the observation period up to 52 weeks of age. Both the fetal and adult compound-deficient mice showed a reduction in the trabecular bone volume with suppressed bone formation, but normal bone resorption, whereas the single deficient mice (*Bmp2*+/− or *Bmp6*−/−) did not. When a fracture was created at the femoral midshaft and the bone healing was analyzed, the endochondral bone formation, but not intramembranous bone formation, was impaired by the compound deficiency. In the cultures of bone marrow cells, however, there was no difference in osteogenic differentiation between WT and compound-deficient cells in the presence or absence of the exogenous BMP2. We thus concluded that endogenous BMP2 and BMP6 cooperatively play pivotal roles in bone formation under both physiological and pathological conditions.

Bone morphogenetic proteins (BMPs)[2] are members of secreted signaling proteins that belong to the transforming growth factor-β superfamily. BMPs were originally identified as molecules that induced ectopic bone formation when implanted into rodent muscles (1, 2). In accordance with such *in vivo* effects, BMPs have been shown to regulate osteogenic differentiation *in vitro* (3). However, naturally occurring or genetically engineered mice deficient in BMPs reported so far are either normal, exhibit abnormalities in skeletal patterning, or die during early embryonic development, thus being non-informative as to the role of endogenous BMPs in bone formation (4, 5).

In mammals, there are two distinct modes of bone formation: intramembranous and endochondral (6). Most of the bones form through the latter process, which is characterized by the replacement of a cartilage mold by bone and bone marrow (7). During this process, cells in the mesenchymal condensations become chondrocytes, the primary cell type of cartilage; cells at the border of the condensations form a perichondrium. Chondrocytes have a characteristic shape, express a characteristic genetic program driven by SOX9 and other transcription factors, and secrete a matrix rich in type II collagen and proteoglycan. Cartilage enlarges through chondrocyte proliferation and matrix production. Chondrocytes in the center of the cartilage mold then stop proliferating, enlarge (hypertrophy), and change their genetic program to synthesize the type X collagen. Hypertrophic chondrocytes mineralize their surrounding matrix, attract blood vessels through the production of the vascular endothelial growth factor and other factors, and attract chondroclasts and osteoclasts. Moreover, these chondrocytes direct mesenchymal cells in the perichondrium and in the bone marrow to become osteoblasts, which form the bone collar and the primary spongiosa (8, 9). Thus, during the endochondral bone formation, hypertrophic chondrocytes link chondrogenesis to osteogenesis by inducing osteogenesis and angiogenesis (8, 9). Hypertrophic chondrocytes express a number of growth factors, cytokines, and matrix proteins. Among them, Indian hedgehog (Ihh) has been proven to be indispensable for the induction of osteogenesis by these chondrocytes (8, 10). Ihh alone, however, cannot induce bone formation (11), suggesting that other factors secreted from these chondrocytes may also be necessary for osteogenesis. Because some BMPs can induce ectopic bone formation when implanted into rodent muscles and promote osteogenic differentiation *in vitro*, they are strong candidates for the osteogenic factors secreted by these chondrocytes. Among them, BMP2 and BMP6 are known to be expressed by these chondrocytes (8). As is the case with the other BMPs, however, there is no direct evidence that the endogenous BMP2 and BMP6 are involved in bone formation, because homozygous *Bmp2*-deficient (*Bmp2*−/−) mice die during the early embryonic stage (12), and homozygous *Bmp6*-deficient (*Bmp6*−/−) mice show no skeletal abnormality except for a slight delay in the ossification of the sternum (13). We hypothesized that there might be a genetic redundancy between BMP2 and BMP6 in the regulation of bone formation. Hence, the present study generated compound knock-out mice lacking one allele of the *Bmp2* gene and both alleles of the *Bmp6* gene (*Bmp2*+/−; *Bmp6*−/−) and investigated the effect of their compound loss on bone metabolism under both physiological and pathological conditions.

EXPERIMENTAL PROCEDURES

Animals—*Bmp2*+/− mice were kindly provided by A. Bradley (Baylor College of Medicine, Houston, TX) (12); *Bmp6*−/− mice by E. Robertson (Harvard University, Cambridge, MA) (13). The mice were maintained in a C57BL/6 background. To generate *Bmp2*+/−;

* This work was supported by Grant-in-aid for Scientific Research 16659400 from the Japanese Ministry of Education, Culture, Sports, Science, and Technology. The costs of publication of this article were defrayed in part by the payment of page charges. This article must therefore be hereby marked "*advertisement*" in accordance with 18 U.S.C. Section 1734 solely to indicate this fact.

[1] To whom correspondence should be addressed. Tel.: 81-3-3815-5411 (ext. 37014 or 33376); Fax: 81-3-3818-4082; E-mail: uichung-tky@umin.ac.jp.

[2] The abbreviations used are: BMP, bone morphogenetic protein; Ihh, Indian hedgehog; WT, wild type; RT, reverse transcriptase; BMD, bone mineral density; rh, recombinant human; ALP, alkaline phosphatase; CFU, colony forming unit; MMP-13, metalloproteinase 13.

Bmp6−/− mice, *Bmp2*+/− mice were mated with the homozygous *Bmp6*−/− mice to obtain *Bmp2*+/−;*Bmp6*+/− mice. *Bmp2*+/−; *Bmp6*+/− mice were then mated with each other. Because *Bmp2*−/− mice were embryonically lethal, two of 12 live mice were expected to be *Bmp2*+/−;*Bmp6*−/−. All experiments were performed on male mice in accordance with the protocol approved by the Animal Care and Use Committee of the University of Tokyo.

Genotyping—Genomic DNA was isolated from the tail. 10 ng of genonic DNA was used for genotyping by PCR. The PCR primers were as follows: 5′-AGCATGAACCCTCATGTGTTGG-3′ (forward primer for *Bmp2* wild-type (WT) and mutant alleles), 5′-GTGACATTAGGCTGCTGTAGCA-3′ (reverse primer for *Bmp2* WT allele), 5′-GAGACTAGTGAGACGTGCTACT-3′ (reverse primer for *Bmp2* mutant allele), 5′-TCCCCACATCAACGACAC-3′ (forward primer for *Bmp6* WT and mutant alleles), 5′-TCCCCACCACACAGTCCTTG-3′ (reverse primer for *Bmp6* WT allele) and 5′-CGCTGACAGCCGGAACACGG-3′ (reverse primer *Bmp6* mutant allele). PCR were performed at 94 °C for 1 min, at 58 °C for 1 min, and at 72 °C for 1 min for 35 cycles. The PCR product from the WT *Bmp2* allele was 322 bp and that from the *Bmp2* mutant allele, 367 bp. The PCR product from the WT *Bmp6* allele was 112 bp and that from the *Bmp6* mutant allele, 499 bp.

Skeletal Preparation—Embryos at E17.5 were eviscerated, fixed in 100% ethanol for 4 days, and then transferred to 100% acetone. After 3 days, they were rinsed with water and stained for 10 days in staining solution containing 1 volume of 0.1% Alizarin red S (Sigma), 95% ethanol; 1 volume of 0.3% Alcian blue 8GX (Sigma), 70% ethanol; 1 volume of 100% acetic acid, and 17 volumes of 100% ethanol. After rinsing with 96% ethanol, the specimens were kept in 20% glycerol, 1% KOH at 37 °C for 16 h and subsequently at room temperature until the skeletons became clearly visible. For storage, the specimens were transferred to 50, 80, and finally 100% glycerol (14).

Histological Analysis—For the histological analysis, embryonic limbs were fixed in 4% paraformaldehyde/phosphate-buffered saline for 1 h and embedded in paraffin for sectioning, according to the standard procedures. Sections (5 μm thick) were then stained with Hematoxylin and Eosin (H&E) for morphological study, with toluidine blue for detection of the cartilage matrix, or with 5% silver nitrate for detection of mineralization (the von Kossa method), then mounted in xylene-based media, and photographed. For immunohistochemistry, after treatment with 25 μg/ml hyaluronidase for 1 h at 37 °C, the sections were incubated with monoclonal rat anti-mouse antibodies against the type I, II, and X collagens (LSL, Tokyo, Japan), and MMP-13 (CHEMICON International, Inc., Temecula, CA) for 12–24 h at 4 °C. To visualize the immunoreactivity for type I, II, and X collagens using fluorescence, the sections were incubated with the Alexa 488 anti-rabbit IgG antibody (Molecular Probes) for 1 h at room temperature. To visualize the immunoreactivity for MMP-13, the sections were incubated with the horseradish peroxidase-conjugated goat antibodies against rabbit IgG (ICN Biomedicals, Inc., Aurora, OH) for 20 min at room temperature, immersed in a diaminobenzidine solution for 10 min at room temperature, then counterstained with methylgreen. As a control, rabbit nonimmune serum (Upstate Biotechnology, Charlottesville, VA) was used at the same dilution instead of the primary antibody. To quantify the areas of interest, NIH Image was used to measure the ratio to the total area.

In Situ Hybridization—Tissues were fixed in 4% paraformaldehyde/phosphate-buffered saline overnight at 4 °C, processed, embedded in paraffin, and cut. The *in situ* hybridization was performed as previously described (15) using complementary ^{35}S-labeled riboprobes for mouse BMP2, BMP4, BMP6, BMP7, GDF5 (kindly provided by E. Robertson, Harvard University) (13), and type I collagen (8).

Real-time RT-PCR—Total RNA was extracted using an ISOGEN Kit (Wako Pure Chemicals Industry, Ltd., Tokyo) and an RNeasy Mini Kit (Qiagen, Hilden, Germany), then treated with DNase I (Qiagen), according to the manufacturer's instructions. One μg of RNA was reverse transcribed using a Takara RNA PCR Kit (AMV) version 2.1 (Takara Shuzo Co., Shiga, Japan) to generate the single-stranded cDNA. PCR was performed with the ABI Prism 7000 Sequence Detection System (Applied Biosystems, Foster City, CA). Each PCR consisted of 1× QuantiTect SYBR Green PCR Master Mix (Qiagen), 0.3 μM specific primers, and 500 ng of cDNA. The mRNA copy number of a specific gene in the total RNA was calculated with a standard curve generated using serially diluted plasmids containing PCR amplicon sequences and normalized to the human or rodent total RNA (Applied Biosystems) with mouse actin as the internal control. Standard plasmids were synthesized using a TOPO TA Cloning Kit (Invitrogen, Carlsbad, CA), according to the manufacturer's instructions. All reactions were run in triplicate. The primer sequences are available upon request.

Radiological Analysis—Bone radiographs were taken with a soft x-ray instrument (CMB-2, SOFTEX, Kanagawa, Japan). A three-dimensional CT scan was taken with a composite x-ray analyzing system (NX-HCP, NS-ELEX Inc., Tokyo). The bone mineral density (BMD) was measured by single energy x-ray absorptiometry using a bone mineral analyzer (DCS-600R, Aloka Co., Tokyo).

Bone Histomorphometry—Eight 9-week-old mice were used in each group. For Villanueva-Goldner staining, tibias were fixed with ethanol, embedded in methyl methacrylate, and sectioned in 6-μm slices. For double labeling, the mice were subcutaneously injected with 8 mg/kg body weight of calcein at 3 and 10 days before sacrifice. Tartrate-resistand acid phosphatase-positive cells were stained at pH 5.0 in the presence of L-(+)-tartaric acid with naphthol AS-MX phosphate (Sigma) in *N,N*-dimethyl formamide as the substrate. The specimens were subjected to histomorphometric analyses using an image analyzer (Histometry RT CAMERA, System Supply Co., Nagano, Japan). The parameters of the trabecular bone were measured in an area 1.2 mm in length from 0.5 mm below the growth plate at the proximal metaphysis of the tibias. The parameters of the cortical bone were measured at the midshaft of the tibias. The thickness of the growth plate was measured at the proximal tibias.

Fracture Model—Bone fractures were generated as previously described (16). Eight 9-week-old mice were used in each group. Briefly, under general anesthesia with xylazine (0.05 mg/10 g body weight) and ketamine (0.5 mg/10 g body weight, Sigma), a 15-mm incision was longitudinally made to expose the femur. A transverse osteotomy was performed with a bone saw (Volvere GX, NSK Nakanishi, Inc., Tochigi, Japan) at the middle of the femur. Fractured bones were repositioned, and then the full-length of the bone marrow cavity was internally stabilized with an intramedullary nail with the inner pin of a 23-gauge spinal needle. The animals were allowed activity, diet, and water *ad libitum*. For the histological analyses, the animals were killed at 5, 7, and 18 days after surgery by asphyxiation with carbon dioxide, and their femurs were excised. The calcified area and the bone mineral content of the entire femur were measured. The % gain of calcified area and the % gain of BMC were calculated, and the differences were compared between WT, *Bmp2*+/−, *Bmp6*−/−, and *Bmp2*+/−;*Bmp6*−/− mice. To distinguish between the intramembranous bone formation and endochondral bone formation during fracture healing, the callus was divided into three equal portions along the axis of the bone. The distal and proximal portions, where bones mainly form through the intramembranous

process (17), were designated as the peripheral part, and the middle portion, where bones mainly form through the endochondral process (17), was designated as the central part. In each part, we measured the ratio of the calcified area to the total area of the histological sections using NIH Image.

Serum and Urinary Biochemistry—Blood samples from 9-week-old WT and *Bmp2+/−;Bmp6−/−* mice ($n = 6$ for each group) were collected by heart puncture under anesthesia with nembutal (0.4 mg/10 g body weight) (Dainippon Pharmaceutical Co., Ltd., Tokyo). Urine samples were collected for 24 h before sacrifice in oil-sealed bottles in the metabolism cages (CL-0305, CLEA Japan, Inc., Tokyo). The levels of creatinine, calcium, and inorganic phosphorus in the serum were measured using a standard colorimetric technique, a Calcium HR Kit (Wako Pure Chemical Industries, Ltd.), and an Inorganic Phosphorus II Kit (Wako Pure Chemical Industries, Ltd.), respectively, by an autoanalyzer (Type 7170, Hitachi High-Technologies Co., Tokyo). Urinary deoxypyridinoline was measured using a Pyriliks-D enzyme-linked immunosorbent assay kit (Metra Biosystems, Inc., Mountain View, CA). The values were corrected for urinary creatinine measured by a standard colorimetric technique using the Type 7170 autoanalyzer.

In Vitro Bone Marrow Differentiation Assay—Bone marrow cells were isolated from WT and *Bmp2+−;Bmp6−/−* mice at 3 weeks of age and inoculated at a density of 2×10^5 cells/well onto 24-well plates in α-minimal essential medium containing 50 μg/ml ascorbic acid, 10 mM β-glycerophosphate, and ITS+1 liquid media supplement (×100) (Sigma) (osteogenic medium). For treatment with BMP, we added recombinant human (rh) BMP2 at 200 ng/ml. We changed the medium every 4 days with BMP2 being replenished each time. Two weeks after confluence, total RNA was extracted, and alkaline phosphatase (ALP), Alizarin red S, and von Kossa stainings were performed. For ALP staining, cells were fixed in 70% EtOH and stained for 10 min with a solution containing 0.01% naphtol AS-MX phosphate disodium salt (Sigma), 1% *N,N*-dimethyl formamide (Wako Pure Chemicals Industry, Ltd.), and 0.06% fast blue BB (Sigma). For the Alizarin red S staining, the cells were fixed in 10% formalin/phosphate-buffered saline and stained for 10 min with 2% Alizarin red S, pH 4.0, (Sigma) solution. For the von Kossa staining, the cells were fixed with 100% ethanol at room temperature for 15 min, stained with 5% silver nitrate solution (Wako Pure Chemicals Industry, Ltd.) under ultraviolet light for 10 min, and incubated for 5 min with 5% sodium thiosulfate solution (Wako Pure Chemicals Industry, Ltd.).

The numbers of total fibroblastic colonies (CFU-F), ALP positive colonies (CFU-ALP), and bone nodules were assessed as described (18–20). In brief, bone marrow cells isolated from WT and *Bmp2+/−; Bmp6−/−* mice at 3 weeks of age were disseminated into a six-well plate at a concentration of 5×10^5 cells/ml and cultured in osteogenic medium for 5, 10, and 15 days in the presence or absence of rhBMP2 at 200 ng/ml. Subsequently, cells were fixed with 10% neutral-buffered formalin and subjected to the ALP or von Kossa stainings as described above. Colonies consisting of more than 50 cells were defined as CFU-F, and ALP-positive CFU-F were defined as CFU-ALP. Bone nodules were counted on a grid under low power microscopy.

Statistical Analysis—The means of the groups were compared by analysis of variance, and the significance of differences was determined by post-hoc testing using Bonferronis method.

RESULTS

BMP Subtypes Expressed by Hypertrophic Chondrocytes—To determine the BMP subtypes expressed by hypertrophic chondrocytes, we performed *in situ* hybridization for BMPs known to be expressed in chondrocytes (5). Consistent with the previous report (8), the main BMP subtypes expressed by hypertrophic chondrocytes were BMP2 and BMP6 (Fig. 1*A*). As for the other BMPs examined, BMP4 was weakly expressed in the prehypertrophic chondrocytes, BMP7 in the proliferating chondrocytes, and GDF5 in the periarticular proliferating chondrocytes.

Analysis of Fetal Bmp2−/−;Bmp6−/− Mice—To investigate the roles of the enodogenous BMP2 and BMP6 during bone formation, we generated their compound-deficient mice by appropriate mating. Because of the early embryonic lethality of *Bmp2−/−* mice, we studied the bone phenotypes of *Bmp2+/−;Bmp6−/−* mice. To macroscopically visualize bone and cartilage elements, whole embryos at E17.5 were double stained with Alizarin red and Alcian blue (Fig. 1*B*). The staining revealed a normal skeletal patterning in the single deficient (*Bmp2+/−* and *Bmp6−/−*) and the compound-deficient mice. However, the size of the compound-deficient mice was smaller than that of WT mice, whereas that of the single deficient mice was not. Temporal profiles of the body length and weight of the compound-deficient mice showed an ~5% decrease in axial growth and body weight throughout life (Fig. 1*C*).

Histological analysis of the growth plate of the proximal tibias from the E17.5 WT and *Bmp2+/−;Bmp6−/−* mice disclosed that the size of the compound-deficient growth plate was smaller than that of WT (643 ± 17 *versus* 723 ± 24 μm, $p < 0.05$), but the proportions of the distinct layers of the growth plate chondrocytes were not significantly different between the two groups (the layer of proliferating chondrocytes, 72.9 ± 2.3 *versus* 72.1 ± 2.6%; the layer of hypertrophic chondrocytes, 27.1 ± 0.8 *versus* 27.9 ± 0.9%) (Fig. 1*D*). Immunohistochemistry of the type II and X collagens showed no remarkable difference between the two groups (Fig. 1*E*).

To evaluate bone formation in the fetal growth plate, we performed immunohistochemistry and real-time RT-PCR detecting the type I collagen (Fig. 1*F*) and von Kossa staining (Fig. 1*G*). The type I collagen immunoreactivity and type I collagen mRNA expression in the tibia were similar between the compound-deficient and WT mice. The von Kossa staining revealed that the mineralized area in the primary spongiosa of the compound-deficient mice was reduced in comparison with that of WT, although the mineralized area in the hypertrophic layer was similar between the two groups. The number of osteoclasts of the compound-deficient mice was not significantly different from that of WT (data not shown). During endochondral bone formation, osteogenesis is influenced by chondrogenesis. To rule out the possibility that the reduced mineralization of the primary spongiosa of the compound-deficient mice was because of a cartilage defect, we investigated whether chondrocytes reached terminal differentiation by examining the onset of hypertrophic differentiation and cartilage mineralization. H&E staining, immunohistochemical analysis with anti-type X collagen and MMP-13 antibodies, and von Kossa staining of the metatarsal bone sections at E15.5 showed that neither hypertrophic differentiation nor cartilage mineralization occurred in WT or compound-deficient mice (Fig. 1*H*). At E16.5, chondrocytes in the center of the cartilage underwent hypertrophic differentiation, expressing type X collagen and mineralizing the surrounding matrix in both WT and *Bmp2+/−; Bmp6−/−* mice. MMP-13, a marker of terminally differentiated hypertrophic chondrocytes (21–23), just began to be expressed in both groups. At E17.5, MMP-13 expression was markedly up-regulated, the area of the mineralized cartilaginous matrix was increased, and the bone collar was formed in both groups. Thus, no abnormality of terminal differentiation of the chondrocytes was detected in the compound-deficient mice. Taken together, these data suggest that the differentiation/

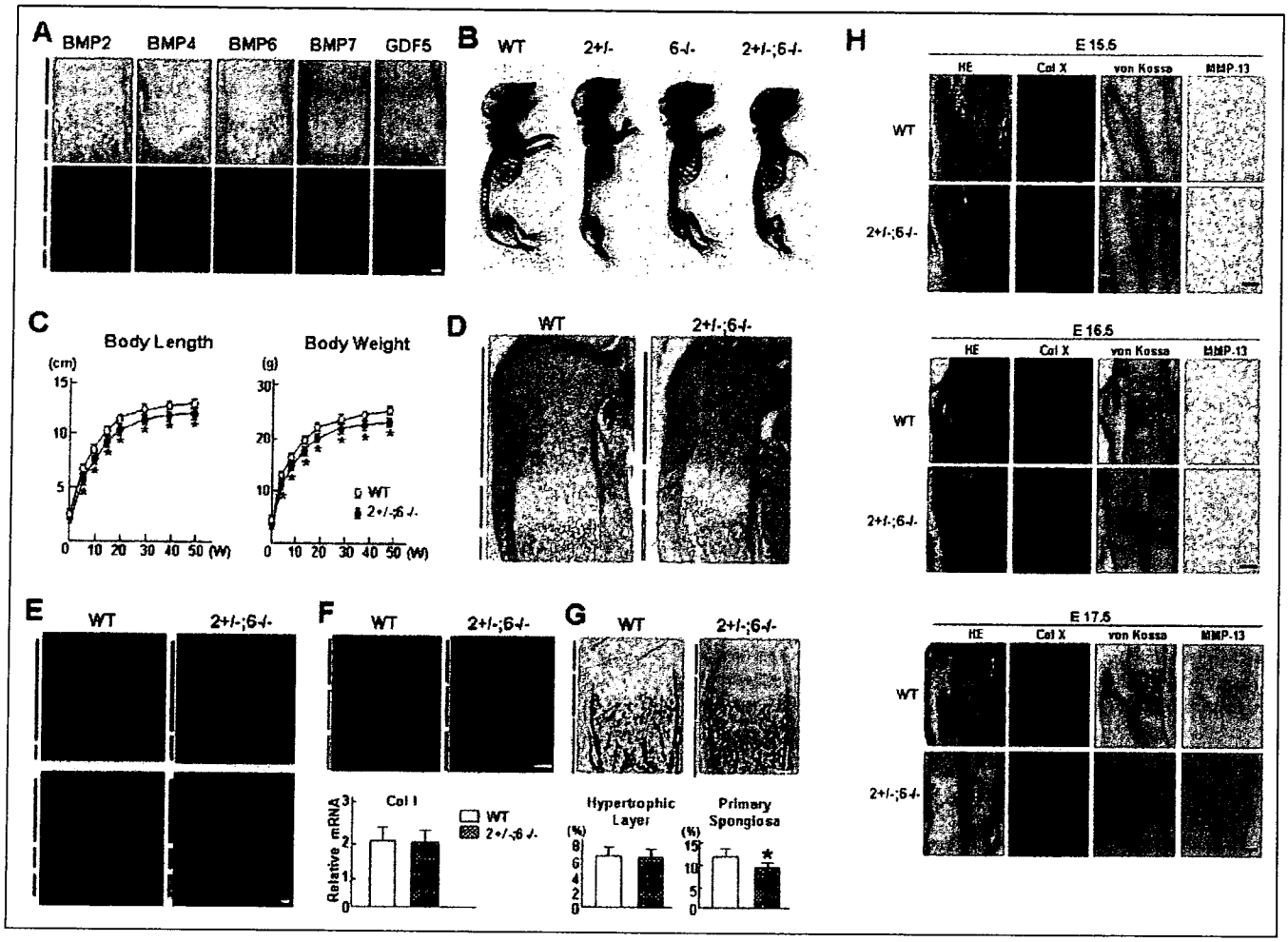

FIGURE 1. **Macroscopic and histological analyses of fetal *Bmp2+/−;Bmp6−/−* mice.** *A*, *in situ* hybridization of the radius growth plates from E17.5 WT mice with mouse BMP2, BMP4, BMP6, BMP7, and GDF5 antisense probes. *Upper panels*, bright field views; *lower panels*, dark field views. *Blue*, *green*, and *red bars* indicate the layer of proliferating chondrocytes, the layer of hypertrophic chondrocytes, and the primary spongiosa, respectively. *Scale bar*, 100 μm. *B*, double staining with Alizarin red and Alcian blue of the whole body from E17.5 WT, *Bmp2+/−*, *Bmp6−/−*, and *Bmp2+/−;Bmp6−/−* mice. *C*, temporal growth profiles of WT and *Bmp2+/−;Bmp6−/−* mice at 0, 5, 10, 20, 30, 40, and 50 weeks of age expressed by the body length from nose to tail and body weight. Data are expressed as mean ± S.E. for 12 mice per group. *, $p < 0.05$ *versus* WT. *D*, H&E staining of the tibia sections from E17.5 WT and *Bmp2+/−;Bmp6−/−* mice. *Blue*, *green*, and *red bars* indicate the layer of proliferating chondrocytes, the layer of hypertrophic chondrocytes, and the primary spongiosa, respectively. *Scale bar*, 100 μm. *E*, immunohistochemical analysis of the tibia sections from E17.5 WT and *Bmp2+/−;Bmp6−/−* mice with anti-type II collagen (*upper panels*) and type X collagen (*lower panels*) antibodies. *Blue*, *green*, and *red bars* indicate the layer of proliferating chondrocytes, the layer of hypertrophic chondrocytes, and the primary spongiosa, respectively. *Scale bar*, 100 μm. *F*, immunohistochemical analysis with anti-type I collagen antibody of the tibia sections from E17.5 WT and *Bmp2+/−;Bmp6−/−* mice (*upper panels*). Real-time RT-PCR analysis of type I collagen mRNA expression in the tibias from E17.5 WT and *Bmp2+/−;Bmp6−/−* mice (*lower panels*). *Blue*, *green*, and *red bars* indicate the layer of proliferating chondrocytes, the layer of hypertrophic chondrocytes, and the primary spongiosa, respectively. *Scale bars*, 100 μm. *G*, von Kossa staining of the tibia sections from E17.5 WT and *Bmp2+/−;Bmp6−/−* mice (*upper panels*). The relative ratio of the calcified area in the hypertrophic layer and that in the primary spongiosa were histologically measured (*lower panels*). *Blue*, *green*, and *red bars* indicate the layer of proliferating chondrocytes, the layer of hypertrophic chondrocytes, and the primary spongiosa, respectively. *Scale bars*, 100 μm. Data are expressed as the mean ± S.E. of 6 mice per genotype. *, $p < 0.05$ *versus* WT. *H*, H&E staining, immunohistochemical analysis with anti-type X collagen and MMP-13 antibodies and von Kossa staining of the metatarsal bone sections at E15.5, E16.5, and E17.5 from WT and *Bmp2+/−;Bmp6−/−* mice. *Scale bar*, 100 μm.

function of osteoblasts is impaired by the compound deficiency of *Bmp2* and *Bmp6*.

Analysis of Adult Bmp2+/−;Bmp6−/− Mice—We then investigated whether the compound deficiency of *Bmp2* and *Bmp6* had effects on the bone metabolism in adult mice. X-rays of the femur at 9 weeks of age showed that the lengths of the femur and the tibia were shorter and that the trabecular bone volume was reduced in *Bmp2+/−;Bmp6+/−* mice compared with that in WT (Fig. 2*A*). Quantitative analysis of the BMD disclosed that the femoral BMD of the compound-deficient mice was reduced compared with that of WT, whereas that of *Bmp2+/−*, *Bmp6+/−*, *Bmp6−/−*, or *Bmp2+/−;Bmp6+/−* mice was not significantly different from that of WT (Fig. 2*B*). Three-dimensional CT analysis manifested a marked reduction in the trabecular bone volume of the compound-deficient mice (Fig. 2*C*). Next, to investigate the role of endogenous *Bmp2* and *Bmp6* in intramembranous bone formation, the calvarias were examined. X-ray of the calvarias at 9 weeks of age from WT, *Bmp2+/−*, *Bmp6−/−*, and *Bmp2+/−;Bmp6−/−* mice did not show any significant difference (Fig. 2*D*), which was confirmed by the quantitative analysis of the BMD (Fig. 2*E*).

Histological analysis with von Kossa staining of the proximal tibia revealed a trabecular bone loss in *Bmp2+/−;Bmp6−/−* mice compared with that in WT (Fig. 3*A*). Although there was no significant difference in the proportions of the growth plates or in the cartilaginous mineralization between the two groups, the mineralization in the primary spongiosa was notably reduced in the compound-deficient mice (Fig. 3*B*). To analyze the mechanism of the bone loss in detail, bone histomorphometric analysis was performed on the tibias (Fig. 3*C*). The bone volume and cortical thickness of the compound-deficient mice were found to be decreased compared with those of WT. Regarding the parameters of bone formation, the mineral apposition rate and bone

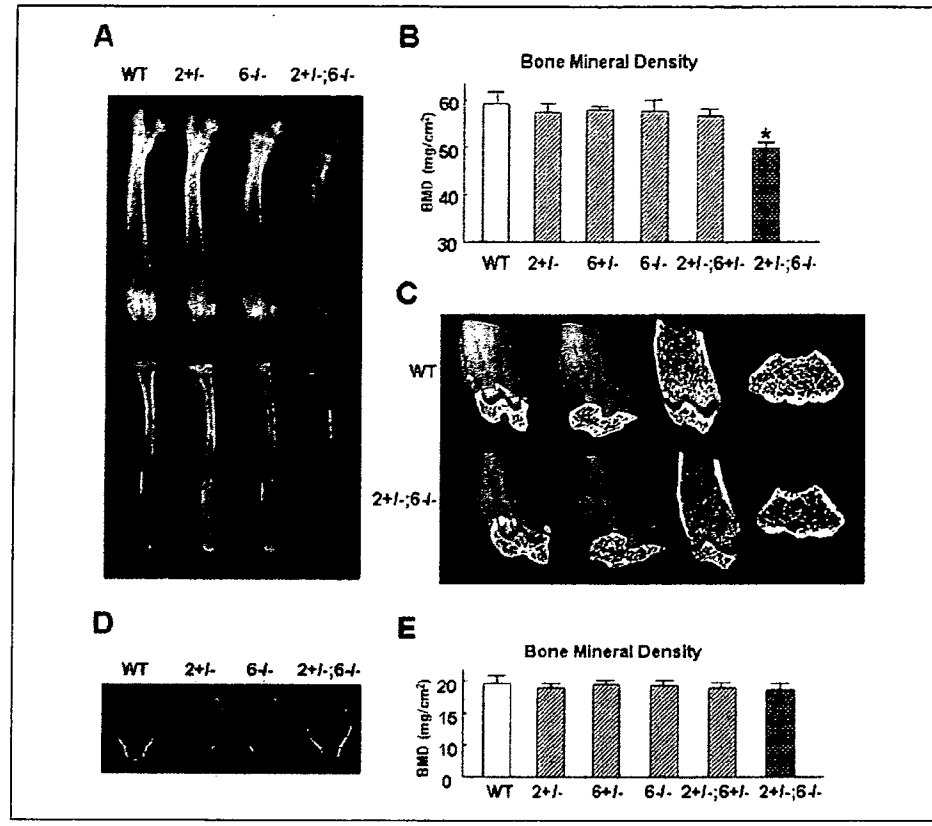

FIGURE 2. **Radiological analysis of adult *Bmp2+/−;Bmp6−/−* mice.** *A*, plain radiographs of the femurs (*upper panels*) and tibias (*lower panels*) from WT, *Bmp2+/−*, *Bmp6−/−*, and *Bmp2+/−;Bmp6−/−* mice at 9 weeks of age. *B*, BMD of the whole femurs from WT, *Bmp2+/−*, *Bmp6+/−*, *Bmp6−/−*, *Bmp2+/−;Bmp6+/−*, and *Bmp2+/−;Bmp6−/−* mice at 9 weeks of age. Data are expressed as mean ± S.E. for 12 bones/group. *, $p < 0.01$ *versus* the rest. *C*, three-dimensional CT analysis of the distal epiphysis of the femurs from WT (*upper panels*) and *Bmp2+/−;Bmp6−/−* mice (*lower panels*) at 9 weeks of age. *D*, plain radiographs of the calvarias from WT, *Bmp2+/−*, *Bmp6−/−*, and *Bmp2+/−;Bmp6−/−* mice at 9 weeks of age. *E*, BMD of the calvarias from WT, *Bmp2+/−*, *Bmp6+/−*, *Bmp6−/−*, *Bmp2+/−;Bmp6+/−*, and *Bmp2+/−;Bmp6−/−* mice at 9 weeks of age.

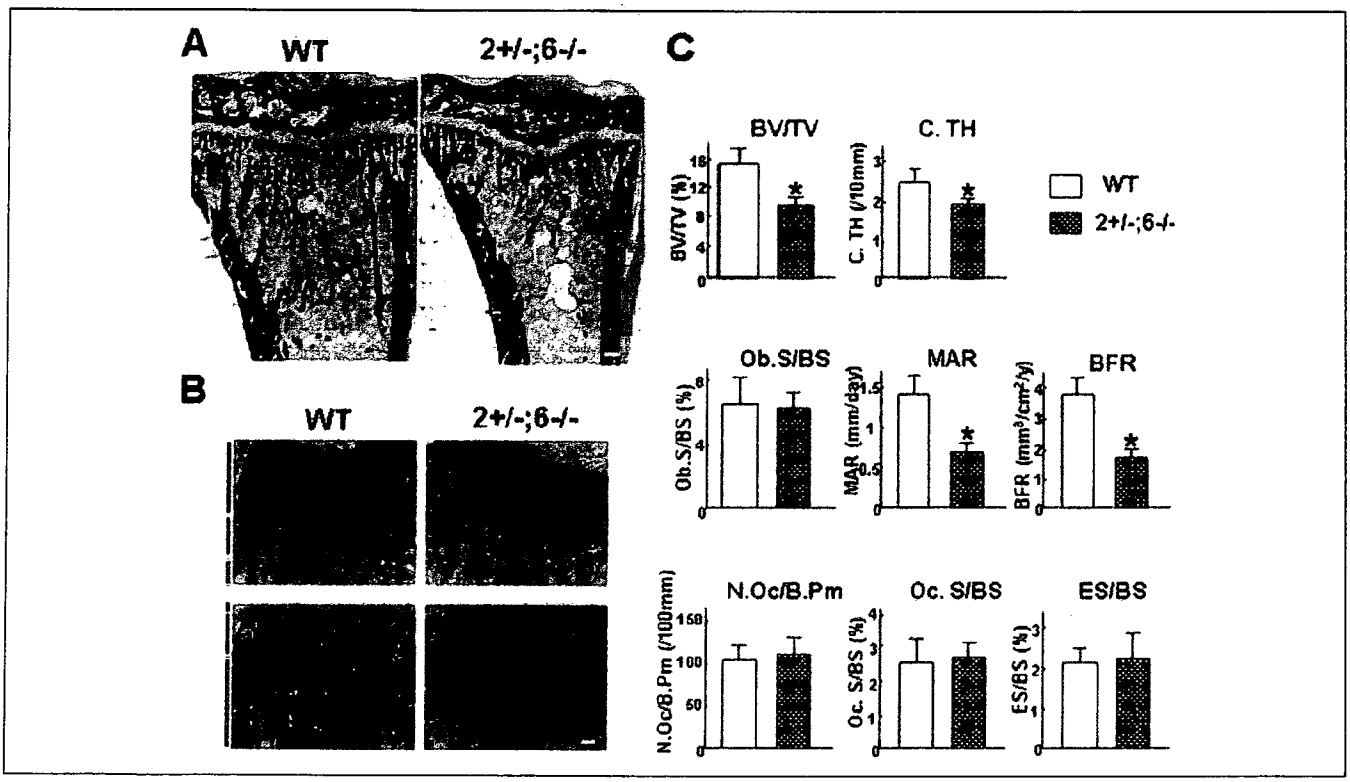

FIGURE 3. **Histological analysis of adult *Bmp2+/−;Bmp6−/−* mice.** *A*, von Kossa staining of the tibia sections from WT and *Bmp2/−;Bmp6−/−* mice at 9 weeks of age. *Scale bar*, 300 μm. *B*, toluidine blue staining (upper panels) and von Kossa staining (*lower panels*) of the tibia growth plate sections from WT and *Bmp2+/−;Bmp6−/−* mice at 9 weeks of age. *Blue*, *green*, and *red bars* indicate the layer of proliferating chondrocytes, the layer of hypertrophic chondrocytes, and the primary spongiosa, respectively. *Scale bar*, 20 μm. *C*, bone histomorphometric analysis of the tibias from WT and *Bmp2+/−;Bmp6−/−* mice at 9 weeks of age. *BV/TV*, bone volume per tissue volume; *C.Th*, cortical bone thickness; *Ob.S/BS*, osteoblast surface per bone surface; *MAR*, mineral apposition rate; *BFR/BS*, bone formation rate per bone surface; *N.Oc/B.Pm*, number of osteoclasts per 100 mm of bone perimeter; *Oc.S/BS*, osteoclast surface per bone surface; *ES/BS*, erosive surface per bone surface. Data are expressed as the mean ± S.E. of 8 mice per genotype. *, $p < 0.05$ *versus* WT.

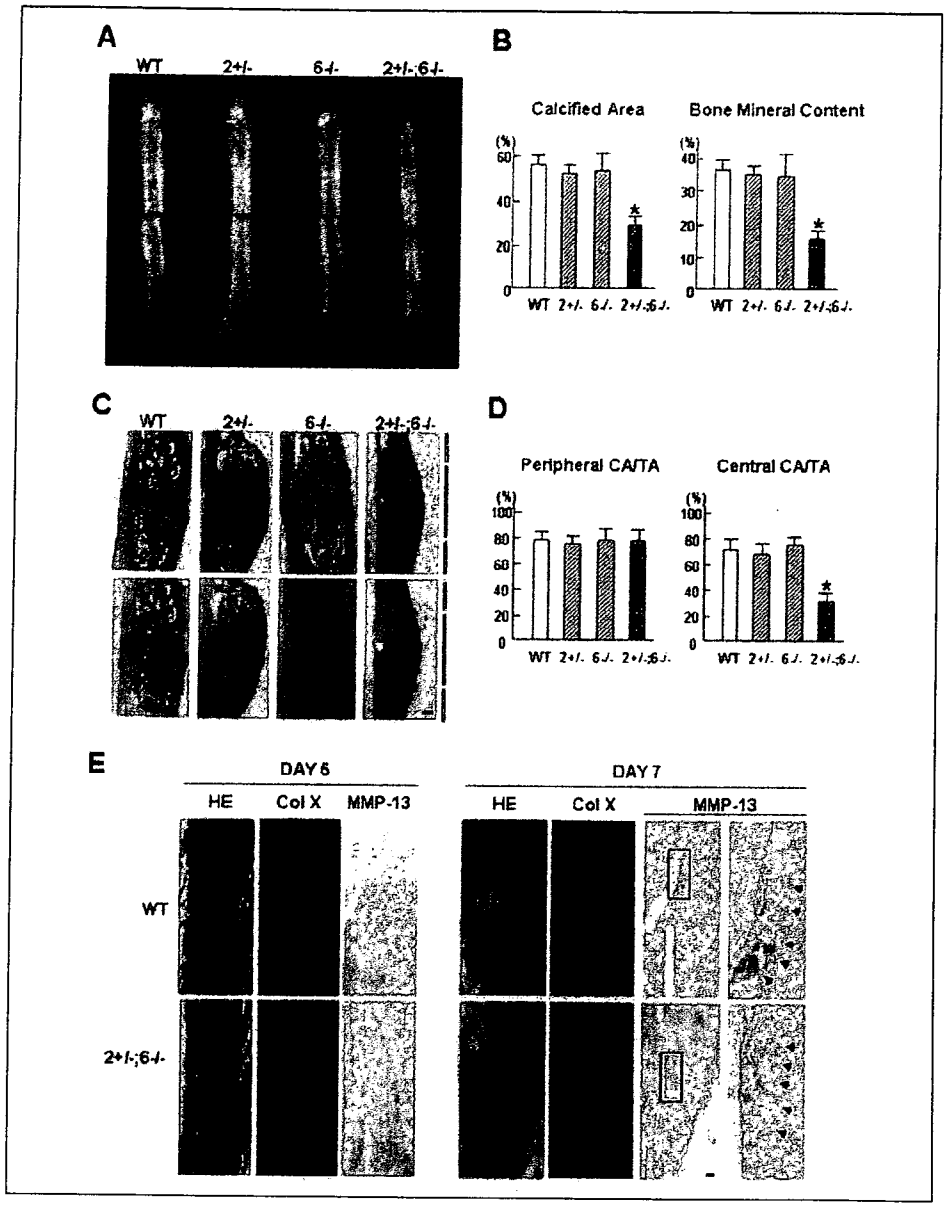

FIGURE 4. **Radiological and histological analyses of the fracture callus.** *A*, plain radiographs of the fractured femurs at 18 days after the surgery from WT, *Bmp2+/−*, *Bmp6−/−*, and *Bmp2+/−*; *Bmp6−/−* mice at 9 weeks of age. *B*, measurement of the calcified area and the bone mineral content of the callus at the fracture site measured by single energy x-ray absorptiometry. Data are expressed as the mean ± S.E. of 8 mice per genotype. *, $p < 0.01$ *versus* WT. *C*, H&E staining (*upper panels*) and toluidine blue staining (*lower panels*) of the fractured femur sections from WT, *Bmp2+/−*, *Bmp6−/−*, and *Bmp2+/−;Bmp6−/−* mice. *Red* and *blue bars* indicate the peripheral part and the central part of the fracture site, respectively. *Scale bar*, 300 μm. *D*, the ratio of the calcified area to the total area (*CA/TA*) in the peripheral part (*left panel*) and central part (*right panel*) of the fracture site histologically measured by NIH Image. Data are expressed as the mean ± S.E. of 8 mice per genotype. *, $p < 0.01$ *versus* WT. *E*, H&E staining and immunohistochemical analysis with anti-type X collagen and MMP-13 antibodies of the sections of the fractured femurs at 5 and 7 days after the surgery from WT and *Bmp2+/−;Bmp6−/−* mice. The *boxed areas* in the *left panels* showing MMP-13 expression are magnified in the *right panels*. *Arrowheads* indicate MMP-13 expression, which is stained *brown*. *Scale bar*, 300 μm.

formation rate per bone surface were markedly decreased with no remarkable difference in the osteoblast number expressed by Ob.S/BS. On the other hand, the parameters of bone resorption were normal. These data suggest that the bone loss in the compound-deficient mice is caused by the inhibition of the bone formation because of the impaired osteoblast function.

To rule out the possibility that the bone loss of these mice was caused by general conditions, such as renal failure or abnormal calcium homeostasis, the serum biochemical data were analyzed. There was no remarkable difference in the serum creatinine, calcium, or inorganic phosphorus between WT and compound-deficient mice (data not shown). Urinary deoxypyridinoline, a marker for bone resorption, showed no remarkable difference between the two groups, confirming the bone histomorphometric data (data not shown).

Bone Fracture Healing in Bmp2+/−;Bmp6−/− Mice—The data so far suggest that the combination of the endogenous BMP2 and BMP6 plays an important role in bone formation under physiological conditions. To further investigate the effects of the compound loss of *Bmp2* and *Bmp6* on bone formation under pathological conditions, we generated fractures at the midshaft of the femurs and compared the healing process among WT, *Bmp2+/−*, *Bmp6−/−*, and *Bmp2+/−;Bmp6−/−* mice. Radiological analysis at 18 days after the fracture showed substantial calcified callus formation in WT, *Bmp2+/−*, and *Bmp6−/−* mice (Fig. 4*A*). On the other hand, in the compound-deficient mice, fracture healing was delayed, and the size of the calcified callus was reduced. To quantify the extent of the callus formation, the % gain of the calcified area and the % gain of bone mineral content in the fractured and control femurs were measured using a bone densitometer (Fig. 4*B*). Although no significant difference was observed among WT, *Bmp2+/−*, and *Bmp6−/−* mice at 18 days after the fracture, both parameters were markedly reduced in the compound-deficient mice. When histological sections were stained with H&E and toluidine blue to distinguish between the bone and cartilage tissues, the total callus size was reduced, and a massive cartilaginous callus containing hypertrophic chondrocytes persisted in the compound-deficient mice. During fracture healing, new bone is known to be formed through two pathways: the endo-

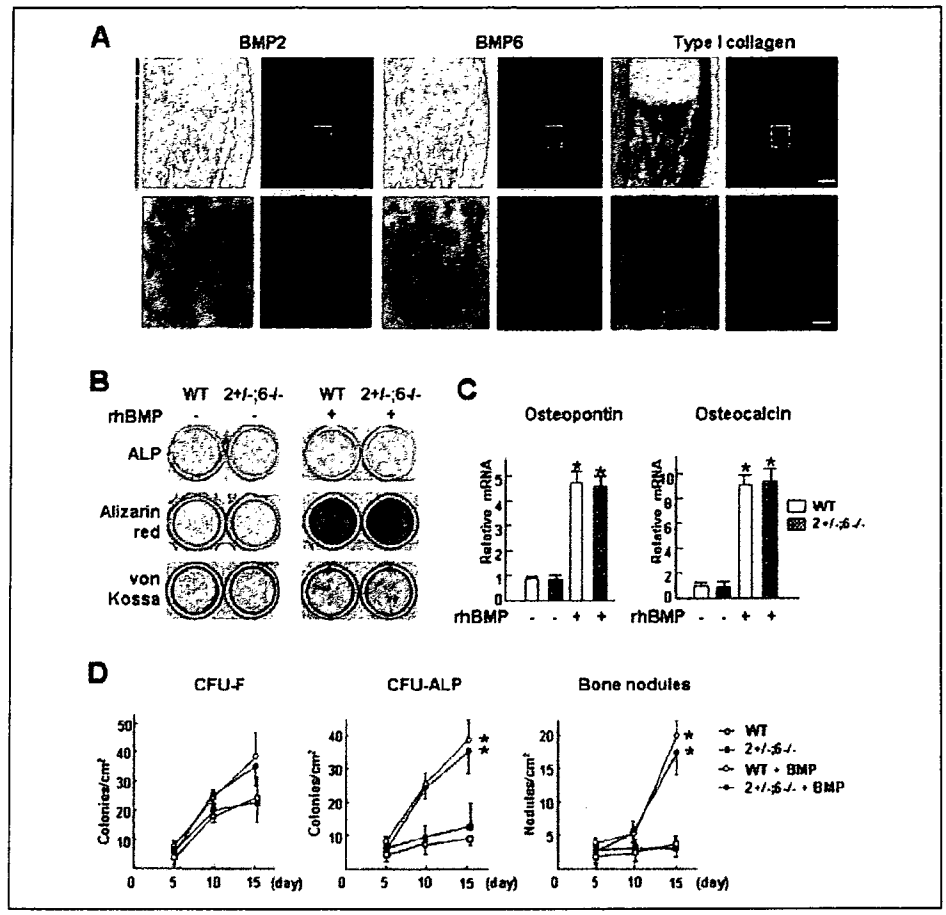

FIGURE 5. **Osteogenic differentiation in the cultures of *Bmp2+/−;Bmp6−/−* bone marrow cells.** *A, in situ* hybridization of the tibia sections from WT mouse with mouse BMP2, BMP6, and type I collagen antisense probes. *Left panels*, bright field views; *right panels*, dark field views. *Blue, green,* and *red bars* indicate the layer of proliferating chondrocytes, the layer of hypertrophic chondrocytes, and the primary and secondary spongiosas, respectively. *Lower panels* are the magnified views of the *boxed areas* in the *upper panels*. *Scale bar*, 100 μm in the *upper panels* and 20 μm in the *lower panels*. *B*, bone marrow cells were isolated from 3-week-old WT and *Bmp2+/−; Bmp6−/−* mice and cultured in serum-free osteogenic medium in the presence or absence of exogenous rhBMP2 (200 ng/ml). Two weeks after confluence, ALP, Alizarin red S, and von Kossa stainings were performed. *C*, expression of osteopontin and osteocalcin mRNAs was determined by real-time RT-PCR on the above mentioned marrow cells. Data are expressed as the mean ± S.E. of 6 wells per group. *, $p < 0.01$, significant stimulation by rhBMP2. *D*, temporal profiles of the numbers of CFU-F, CFU-ALP, and bone nodules using WT and *Bmp2+/−;Bmp6−/−* bone marrow cells. Bone marrow cells were isolated from 3-week-old mice, then cultured in serum-free osteogenic medium in the presence or absence of exogenous rhBMP2 (200 ng/ml). After 5, 10, and 15 days, ALP and von Kossa stainings were performed. Data are expressed as mean ± S.E. for 6 wells per group. *, $p < 0.01$, significant stimulation by rhBMP2.

chondral bone formations in the center and the intramembranous bone formation in the periphery of the callus (17). To distinguish these two pathways, we divided the callus into three equal portions along the axis of the bone, and designated the distal and proximal ⅓ portions as the peripheral part, and the middle ⅓ portion as the central part. The measurement of the ratio of the calcified area to the total area (CA/TA) of the histological sections using NIH Image revealed that calcification in the central part, but not in the peripheral part, was significantly reduced in the compound-deficient mice compared with that in WT (Fig. 4*D*), indicating that the endochondral, not intramembranous, bone formation, was defective in the compound-deficient mice. To investigate whether the delayed fracture healing in *Bmp2+/−;Bmp6−/−* mice was caused by a delay in terminal differentiation of chondrocytes, we examined the earlier stages of fracture healing in WT and compound-deficient mice. H&E staining and immunohistochemical analysis with anti-type X collagen and MMP-13 antibodies showed that no hypertrophic differentiation occurred in either group at 5 days after the fracture (Fig. 4*E*). At 7 days after the fracture, terminal hypertrophic differentiation of chondrocytes determined by expression of MMP-13 and intramembranous bone formation occurred in both groups.

In Vitro Bone Marrow Differentiation Assay—The current results support the view that the endogenous BMP2 and BMP6 play vital roles in bone formation under physiological and pathological conditions. *In situ* hybridization analysis indicated that, in comparison with the expression in hypertrophic chondrocytes, there was little, if any, expression of BMP2 and BMP6 in bone and bone marrow cells including osteoblasts that were marked by the strong expression of the type I collagen (Fig. 5*A*). However, we still could not rule out the possibility that a small amount of BMP2 and BMP6 secreted from bone and bone marrow cells might act in an autocrine or paracrine fashion to modulate the osteoblast function. To test this possibility, we isolated bone marrow cells including osteoblasts from 3-week-old mice, cultured them in serum-free osteogenic medium, and assessed their osteogenic ability. ALP, Alizarin red S, and von Kossa stainings revealed no difference in the basal osteogenic ability between WT and *Bmp2+/−;Bmp6−/−* cells (Fig. 5*B*). Upon treatment with rhBMP2 (200 ng/ml), both WT and the compound-deficient cells responded well to the same extent (Fig. 5*B*). The real-time RT-PCR analysis of osteopontin and osteocalcin, markers for osteoblasts, revealed no difference between the two genotypes (Fig. 5*C*). The quantitative analysis of the numbers of CFU-F, CFU-ALP, and bone nodules using bone marrow cells isolated from 3-week-old WT and compound-deficient mice revealed no difference in the basal osteogenic ability (Fig. 5*D*). Upon treatment with rhBMP2 (200 ng/ml), both WT and the compound-deficient cells responded well to the same extent in terms of the numbers of CFU-ALP and bone nodules (Fig. 5*D*). These data suggest that the endogenous BMP2 and BMP6 secreted from bone marrow cells do not contribute to the regulation of bone formation.

DISCUSSION

Because hypertrophic chondrocytes induce bone formation in the primary spongiosa and the perichondrium during endochondral bone formation, the present study hypothesized that endogenous BMPs secreted from these chondrocytes might be involved in bone formation. Although there have been a number of reports describing the expression patterns of BMPs in the growth plate (13), they do not particularly

focus on these chondrocytes. To obtain physiologically relevant data on the role of the endogenous BMPs during bone formation, we screened for BMPs expressed by these chondrocytes to find that BMP2 and BMP6 were the main subtypes and analyzed the effects of their loss on bone formation.

Fetal *Bmp2+/−;Bmp6−/−* mice exhibited a reduced bone formation in the primary spongiosa, probably because of reduced bone formation and/or stimulation of bone resorption. We think the latter possibility rather unlikely, because the number of osteoclasts was not increased in the compound-deficient mice. The expression of the type I collagen, a marker for both early and late osteoblasts, showed no reduction, suggesting that the differentiation of osteoblasts from the precursor cells was not affected. The growth plates of these mice were smaller, but the proportions of distinct layers were maintained; in addition, the expressions of type II and X collagens were not changed, and hypertrophic chondrocytes mineralized the surrounding cartilaginous matrix to the same extent as WT. There was no difference in the onset of terminal differentiation. These data suggest that there is little, if any, abnormality in the chondrocyte differentiation. The data for adult mice concur with those of fetal mice; bone formation was reduced because of the impaired function of the osteoblasts with no change in their number, whereas the bone resorption markers were all normal. Taken together, these findings provide evidence that the combination of the endogenous BMP2 and BMP6 is vital for bone formation in both the fetal and adult life stages.

In line with our results are those of transgenic mice expressing a dominant-negative form of the *BMP receptor 1B* (*BMPR-1B*) under the control of the type I collagen promoter (24). They were smaller than WT and showed impairment of postnatal bone formation with the number of osteoblasts and the parameters of bone resorption unchanged, suggesting that the osteoblast function was impaired. In addition, transgenic mice lacking the *BMP receptor 1A* (*BMPR-1A*) specifically in osteoblasts using the Cre/loxP system under the control of the Og2 promoter also exhibited a low bone mass because of the impaired osteoblast function (25). The bone phenotypes of these genetically manipulated mice, of which the osteoblast could not transduce normal BMP signaling, are similar to those of *Bmp2+/−;Bmp6−/−* mice. These data suggest that osteoblasts require endogenous BMPs to provide their full function *in vivo*, but are not informative on the subtype and the origin of such BMPs. Our data suggest that BMP2 and BMP6 are two of them.

One question, however, still remained as to where BMP2 and BMP6 came from to act on the osteoblasts. There were three possibilities. First, they came from hypertrophic chondrocytes. Second, they came from bone and bone marrow cells in an autocrine or paracrine fashion. Third, they came from other cell sources at a distance in an endocrine fashion. *In situ* hybridization analysis of the developing bone showed that BMP6 was exclusively expressed in hypertrophic chondrocytes and that BMP2 was strongly expressed in hypertrophic chondrocytes and marginally in the osteoblasts. Bone marrow cells obtained from *Bmp2+/−; Bmp6−/−* mice showed the same osteogenic ability as WT both at the basal status and in response to the exogenous BMP2. Furthermore, intramembranous bone formation in the calvaria was not affected in *Bmp2+/−;Bmp6−/−* mice. These data favor the first possibility. To strictly prove this, however, a further study using the tissue-specific ablation of the *Bmp2* and *Bmp6* genes in hypertrophic chondrocytes is needed. In addition, we should be careful in extrapolating the results of murine experiments to humans, because the growth plate, the source of hypertrophic chondrocytes, in humans disappears at puberty, whereas that of mice persists throughout life.

As for the small size of the growth plate, it may be related to the decreased axial growth of the mutant mice. It may be that the loss of BMP2 and BMP6 affects the size of the mesenchymal condensations and/or the proliferation rate of the chondrocytes. Alternatively, the osteoblast dysfunction caused by the compound loss of these BMPs may elicit a decrease in the axial bone growth, because there is a report that the ablation of the osteoblasts led to skeletal growth arrest (26). A further study is needed to clarify these issues.

In the fracture model, the cartilaginous callus was almost completely replaced by newly formed bone tissue in WT mice, whereas a massive cartilaginous callus persisted in *Bmp2+/−;Bmp6−/−* mice. When the callus was divided into the central and peripheral part, mineralization of the central part, where the endochondral bone formation prevailed, was reduced. These data suggest that the replacement of cartilaginous callus by bone is affected in the compound-deficient mice, which is in line with the data for physiological bone formation. It is noteworthy that the total callus size of the compound-deficient mice was smaller than that of WT. This may be because of the same cause of the smaller size of the growth plate.

A previous study of chimeric mice containing both WT and *Ihh−/−*; parathyroid hormone/parathyroid hormone-related peptide receptor−/− cells revealed that Ihh synthesized by the prehypertrophic and hypertrophic chondrocytes was locally required for the induction of bone formation in the adjacent perichondrium (8). In these chimeric mice, although both BMP2 and BMP6 were strongly expressed by the ectopic *Ihh−/−*;parathyroid hormone/parathyroid hormone-related peptide receptor−/− hypertrophic chondrocytes, the ectopic bone formation did not occur, suggesting that BMPs alone were not sufficient to induce physiological bone formation. In addition, blocking of Hh signaling inhibited the BMP2-induced osteogenic differentiation in mouse limb bud cell line MLB13MYC clone 17 (10), suggesting the presence of synergistic interactions between Ihh and BMPs. In the present study, the lack of one allele of the *Bmp2* gene and both alleles of the *Bmp6* gene caused a reduction in bone formation because of the osteoblast dysfunction. Taken together, we think it likely that BMP2 and BMP6 expressed by hypertrophic chondrocytes act in synergy with Ihh for physiological bone formation.

BMP2 and BMP6 have been reported to form a heterodimer, which was more potent for induction of osteogenic differentiation than the BMP2 homodimer or BMP6 homodimer (27). To assess the role of the BMP2/BMP6 heterodimer *in vivo*, we analyzed the bone formation of *Bmp6−/−* mice. The BMD of *Bmp6−/−* mice, which were thought to have no BMP2/BMP6 heterodimer, was similar to that of WT. In addition, the fracture model did not reveal any difference between WT and *Bmp6−/−* mice. These data suggest that, although the BMP2/BMP6 heterodimer is more potent than the BMP2 or BMP6 homodimers in *in vitro* or implant experiments, the BMP2/BMP6 heterodimer may not have a physiologically relevant role in the bone formation.

In conclusion, the combination of BMP2 and BMP6 plays pivotal roles in bone formation under both physiological and pathological conditions. To the best of our knowledge, this is the first report to show that endogenous BMPs are important for *in vivo* bone formation.

REFERENCES

1. Wozney, J. M., Rosen, V., Celeste, A. J., Mitsock, L. M., Whitters, M. J., Kriz, R. W., Hewick, R. M., and Wang, E. A. (1988) *Science* **242**, 1528–1534
2. Urist, M. R. (1965) *Science* **150**, 893–899
3. Kawabata, M., and Miyazono, K. (2000) in *Skeletal Growth Factors* (Ernesto Canalis, M. D., ed) pp. 269–290, Lippincott Williams & Wilkins, Philadelphia
4. Zhao, G. Q. (2003) *Genesis* **35**, 43–56
5. Karsenty, G. (2000) in *Skeletal Growth Factors* (Ernesto Canalis, M. D., ed) pp. 291–310, Lippincott Williams & Wilkins, Philadelphia
6. Kronenberg, H. M. (2003) *Nature* **423**, 332–336
7. Chung, U. I. (2004) *Endocr. J.* **51**, 19–24

8. Chung, U. I., Schipani, E., McMahon, A. P., and Kronenberg, H. M. (2001) *J. Clin. Investig.* **107**, 295–304
9. Takeda, S., Bonnamy, J. P., Owen, M. J., Ducy, P., and Karsenty, G. (2001) *Genes Dev.* **15**, 467–481
10. Long, F., Chung, U. I., Ohba, S., McMahon, J., Kronenberg, H. M., and McMahon, A. P. (2004) *Development* **131**, 1309–1318
11. Long, F., Zhang, X. M., Karp, S., Yang, Y., and McMahon, A. P. (2001) *Development* **128**, 5099–5108
12. Zhang, H., and Bradley, A. (1996) *Development* **122**, 2977–2986
13. Solloway, M. J., Dudley, A. T., Bikoff, E. K., Lyons, K. M., Hogan, B. L., and Robertson, E. J. (1998) *Dev. Genet.* **22**, 321–339
14. Komori, T., Yagi, H., Nomura, S., Yamaguchi, A., Sasaki, K., Deguchi, K., Shimizu, Y., Bronson, R. T., Gao, Y. H., Inada, M., Sato, M., Okamoto, R., Kitamura, Y., Yoshiki, S., and Kishimoto, T. (1997) *Cell* **89**, 755–764
15. Lee, K., Deeds, J. D., and Segre, G. V. (1995) *Endocrinology* **136**, 453–463
16. Shimoaka, T., Kamekura, S., Chikuda, H., Hoshi, K., Chung, U. I., Akune, T., Maruyama, Z., Komori, T., Matsumoto, M., Ogawa, W., Terauchi, Y., Kadowaki, T., Nakamura, K., and Kawaguchi, H. (2004) *J. Biol. Chem.* **279**, 15314–15322
17. Kawaguchi, H., Kurokawa, T., Hanada, K., Hiyama, Y., Tamura, M., Ogata, E., and Matsumoto, T. (1994) *Endocrinology* **135**, 774–781
18. Aubin, J. E. (1998) *J. Cell. Biochem.* **30–31**, (suppl.) 73–82
19. Malaval, L., and Aubin, J. E. (2001) *J. Cell. Biochem.* **81**, 63–70
20. Nishida, S., Tsurukami, H., Sakai, A., Sakata, T., Ikeda, S., Tanaka, M., Ito, M., and Nakamura, T. (2002) *Bone* **30**, 872–879
21. D'Angelo, M., Yan, Z., Nooreyazdan, M., Pacifici, M., Sarment, D. S., Billings, P. C., and Leboy, P. S. (2000) *J. Cell. Biochem.* **77**, 678–693
22. Jimenez, M. J., Balbin, M., Alvarez, J., Komori, T., Bianco, P., Holmbeck, K., Birkedal-Hansen, H., Lopez, J. M., and Lopez-Otin, C. (2001) *J. Cell Biol.* **155**, 1333–1344
23. Kamekura, S., Hoshi, K., Shimoaka, T., Chung, U., Chikuda, H., Yamada, T., Uchida, M., Ogata, N., Seichi, A., Nakamura, K., and Kawaguchi, H. (2005) *Osteoarthritis Cartilage* **13**, 632–641
24. Zhao, M., Harris, S. E., Horn, D., Geng, Z., Nishimura, R., Mundy, G. R., and Chen, D. (2002) *J. Cell Biol.* **157**, 1049–1060
25. Mishina, Y., Starbuck, M. W., Gentile, M. A., Fukuda, T., Kasparcova, V., Seedor, J. G., Hanks, M. C., Amling, M., Pinero, G. J., Harada, S., and Behringer, R. R. (2004) *J. Biol. Chem.* **279**, 27560–27566
26. Corral, D. A., Amling, M., Priemel, M., Loyer, E., Fuchs, S., Ducy, P., Baron, R., and Karsenty, G. (1998) *Proc. Natl. Acad. Sci. U. S. A.* **95**, 13835–13840
27. Israel, D. I., Nove, J., Kerns, K. M., Kaufman, R. J., Rosen, V., Cox, K. A., and Wozney, J. M. (1996) *Growth Factors* **13**, 291–300

Mod Rheumatol (2006) 16:24–29
DOI 10.1007/s10165-005-0450-6

ORIGINAL ARTICLE

**Noriko Yoshimura · Hirofumi Kinoshita · Noriaki Hori
Taira Nishioka · Masahiko Ryujin · Yoshihiko Mantani
Mariko Miyake · Tatsuya Takeshita · Masao Ichinose
Munehito Yoshiida · Hiroyuki Oka · Hiroshi Kawaguchi
Kozo Nakamura · Cyrus Cooper**

Risk factors for knee osteoarthritis in Japanese men: a case-control study

Received: July 27, 2005 / Accepted: December 13, 2005

Abstract Risk of knee osteoarthritis (OA) was assessed in a population-based case-control study of Japanese men. The study covered three health districts in Wakayama and Osaka prefectures, Japan. Subjects were male individuals ≥45 years old diagnosed radiographically with knee OA, and who did not display any established causes of secondary OA. Controls selected randomly from the general population were individually matched to cases for age, sex, and residential district. Subjects were interviewed using structured questionnaires to determine medical history, physical activity, socio-economic factors, and occupation. Interviews were obtained from 37 cases and 37 controls. In univariate analysis, heaviest weight in the past and physical work such as factory, construction, agricultural, or fishery work as the principal occupation significantly raised the risk of male knee OA ($P < 0.05$). Odds ratios (OR) were determined using conditional logistic regression analysis mutually adjusted for potential risk factors using the results of univariate analysis. Heaviest weight in the past (OR 6.01, 95% confidence interval (CI) 1.18–30.5, $P < 0.05$), past knee injury (OR 6.25, 95% CI 1.13–34.5, $P < 0.05$), and physical work as the principal occupation (OR 6.20, 95% CI 1.40–27.5, $P < 0.05$) represented independent factors associated with knee OA after controlling for other risk factors. Physical work is associated with knee OA, demonstrating the influence of working activity on the development of OA. The present study suggests that risk factors for knee OA in men resemble those in women.

Key words Case control study · Heavy weight · Knee joint · Osteoarthritis (OA) · Physical work

N. Yoshimura (✉) · H. Oka
Department of Joint Disease Research, Graduate School of Medicine, The University of Tokyo, 7-3-1 Hongo, Bunkyo-ku, Tokyo 113-8655, Japan
Tel. +81-3-5800-9178; Fax +81-3-5800-9179
e-mail: yoshimuran-ort@h.u-tokyo.ac.jp

H. Kinoshita
Department of Orthopaedic Surgery, Wakayama Medical University Kihoku Hospital, Wakayama, Japan

N. Hori
Hori Hospital, Sennan, Japan

T. Nishioka
Nishioka Orthopaedic Hospital, Arita, Japan

M. Ryujin
Ryujin Clinic, Wakayama, Japan

Y. Mantani
Tamai Orthopaedic Hospital, Hannan, Japan

M. Miyake
Yamomoto Clinic, Shimotsu, Japan

T. Takeshita
Department of Public Health, Wakayama Medical University School of Medicine, Wakayama, Japan

M. Ichinose
Second Department of Internal Medicine, Wakayama Medical University School of Medicine, Wakayama, Japan

M. Yoshiida
Department of Orthopaedic Surgery, Wakayama Medical University School of Medicine, Wakayama, Japan

H. Kawaguchi · K. Nakamura
Department of Orthopaedic Surgery, Faculty of Medicine, The University of Tokyo, Tokyo, Japan

C. Cooper
MRC Epidemiology Resource Centre, University of Southampton, Southampton General Hospital, Southampton, UK

Introduction

Since osteoarthritis (OA) is a frequent cause of pain and disability in elderly individuals, the recent World Health Organization report on the global burden of disease indicated knee OA as an increasingly important cause of disability in both men and women, suggesting that strategies for preventing OA are urgently required.[1] In Japan, knee OA seems to represent a frequent cause of pain and disability, but few epidemiological studies have examined associated factors.

Several investigations regarding risk factors for hip and knee OA performed in Western populations have

suggested obesity, previous injury, polyarticular joint involvement, and occupational activities as important risk factors for the disorder.[2–8] However, few studies of risk factors for OA in Japanese populations have been performed. Our earlier case-control study of hip OA identified some variations in risk factors in Japan.[9] In the previous case-control study of hip OA, occupational lifting was identified as a risk factor and sedentary work as a protective factor for hip OA. In addition, obesity was not identified as a risk factor for Japanese hip OA. For contrast, an identical case-control study was performed for knee OA in women in a Japanese population.[10] In the female study, risk factors of obesity, previous knee injury, and period of total work were identified, and sedentary work as the initial occupation represented a preventive factor.[10] The results from these two investigations suggest various similarities and differences in risk factors between hip and knee OA in Japanese populations.

The present study sought to clarify risk factors for knee OA among men in Japan, by performing a survey identical to that used in the previous female knee OA study. Results for men were compared to those from the female study.[10] Risk factors were then compared between knee OA and hip OA to address differences in risk factors for constitutional and mechanical factors between OA at different sites. Finally, risk factors for knee and hip OA were compared to those identified in a British study[11,12] that used identical methods to the Japanese studies, to clarify differences in risk factors for OA between Japanese and Western populations.

Patients and methods

Methods of data collection in the present study were basically identical to those of the case-control studies for female knee OA and hip OA reported previously.[9,10] A brief summary is provided here. Cases were identified from the registration systems of the six hospitals participating in the study, which were located in three cities in Japan (Wakayama City and Arita City in Wakayama Prefecture, and Sennan City in Osaka Prefecture).

Cases comprised men ≥45 years old who suffered knee pain and walking difficulties, and who were first diagnosed by an orthopedic surgeon as displaying a tibiofemoral joint with radiographic grade of ≥3 on the Kellgren and Lawrence scale[13] within the year preceding the start of the study. Cases with a history of knee injury in the previous year, rheumatoid arthritis, or ankylosing spondylitis were excluded.

For each case, a single control was randomly selected from among men of the same age and district of residence on city registers of the local population, which are updated as residents move into or leave the city. Controls who had suffered knee OA were excluded from the study.

All eligible cases and controls were initially approached using a letter to determine willingness to participate in the study. After providing informed consent, cases and controls were interviewed by the same trained interviewer.

An identical questionnaire to that used in the British case-control study was used to ascertain risk factors of knee OA.[11,12] The questionnaire was translated and back-translated from Japanese to English. Subjects completed a structured questionnaire that requested details of medical history, socio-economic status and education, cigarette smoking and alcohol consumption, functional status, and lifetime history of leisure activities. Lifetime history of leisure activities included participation in sports such as soccer, swimming, tennis, cricket, and golf, in addition to frequency and duration of less physical activities, such as gardening. Information about eight types of occupational physical activity was requested, namely: standing; sitting; climbing stairs; kneeling; squatting; driving; walking; and heavy lifting. Information on these activities was obtained for the initial job, defined as the earliest job reported, and for the principal job, defined as the job at which the subject had worked longest. For each job, the questionnaire enquired whether work entailed lifting weights (≥10 kg, ≥25 kg, or ≥50 kg) more than once during an average working week. Information regarding use of transport, including frequency and duration of cycling and motorcycling was obtained. Information was also requested on the involvement of other joints, including hands, shoulders, and hips. Furthermore, questions were added about back pain and stiffness, which were not included in the British study. Once heaviest reported weight after 25 years old was obtained, height and weight of each subject was measured at the time of the interview.

After analysis to clarify risk for male knee OA, results were compared between men and published results for women.[10] Risk factors for knee OA and hip OA were also compared to address differences in constitutional and mechanical risk factors between OA at different sites. Finally, risk factors for knee and hip OA were compared to the findings of the British study, which used identical methods to the Japanese studies.

Data were calculated using McNemar's Chi-square test and conditional logistic regression tests for matched sets. Results were summarized as odds ratios (OR) with 95% confidence intervals (CI). Odds ratios were calculated for categories of exposure, and tests of trend were performed across these categories. Statistical analyses were performed using SPSS statistical software (SPSS, Chicago, IL, USA) and the STATA statistical package (STATA, College Station, TX, USA).

Results

A total of 40 men ≥45 years old fulfilled the entry criteria for the study. Among these eligible cases, 37 men (92.5%) agreed to participate after information was provided. Unilateral knee OA ($n = 21$) was more common than bilateral disease ($n = 16$). Among the 21 men with unilateral disease, OA tended to be right-sided ($n = 13$) more often

than left-sided (n = 8), but no significant difference was identified.

For controls, we approached age-, sex-, and residence-matched candidates for each case. To recruit the 37 matched controls, we approached 70 subjects (overall response rate 52.9%).

Table 1 shows background characteristics for the 37 case-control pairs in the present study. Mean body weight was significantly greater for cases than for controls ($P < 0.05$). Furthermore, body mass index was significantly higher for cases than for controls ($P < 0.05$). No differences in personal habits such as smoking or drinking were noted between cases and controls.

The association between knee OA and heaviest reported body weight was analyzed. Under univariate analysis, mean heaviest reported body weight for cases was 72.1 kg (standard deviation (SD) = 13.0 kg), significantly higher than that for controls ($P < 0.01$) in men. Odds ratios for heaviest reported body weight were 1.07 (95% CI 1.02–1.13), suggesting that a 1-kg increase in heaviest reported body weight raised the risk of knee OA by 7%.

To more clearly address the influence of heaviest reported weight on development of knee OA, cases were categorized into the following three groups according to the distribution of heaviest reported weight: high, ≥72.0 kg; middle, 61.0–72.0 kg; and low, <61.0 kg. These categories were defined by dividing total distributions into equal thirds. Cases in the high group displayed a >4-fold elevation in risk compared with cases in the low group (OR 4.22, 95% CI 1.13–15.8 for high vs low, $P < 0.05$; OR 1.60, 95% CI 0.50–5.08 for middle vs low, $P = 0.43$) (Fig. 1).

The association between knee OA and history of injury in other joints was calculated. Under univariate analysis, although ORs exceeded a 2-fold increase, no significant difference was observed between cases and controls (OR 2.50, 95% CI 0.78–7.97 for yes vs no, $P = 0.12$).

The association between knee OA and methods of transportation was examined by comparing the frequency of regular bicycle use between cases and controls. Under univariate analysis, while OR was higher for men (OR 2.67, 95% CI 0.71–10.05), no significant differences were noted between cases and controls.

Associations between knee OA and occupational history were analyzed. The most frequent areas of employment for all subjects were factory/construction, agriculture/fishery, clerical/technical, and shop assistant/manager (Table 2). Distributions of initial and principal occupations differed

Table 1. Anthropometric and background characteristics of cases and controls for knee OA in men

	Men	
	Cases	Controls
No. of participants	37	37
Age (years)	70.0 ± 6.6	70.1 ± 7.0
Weight (kg)	64.1 ± 10.7*	59.3 ± 8.7
Height (cm)	162.5 ± 6.9	163.0 ± 6.7
Body mass index (kg/m^2)	24.2 ± 3.4*	22.4 ± 3.8
Heaviest weight in the past (kg)	72.1 ± 13.0**	64.0 ± 9.2
Age at the heaviest weight (years)	57.4 ± 15.1*	51.7 ± 17.8
Current smoking (%)	16 (43.2)	15 (40.5)
Current drinking (≥5 times/week, %)	20 (54.1)	22 (59.5)

Mean ± SD; percentage in parentheses
* $P < 0.05$, ** $P < 0.01$ cases vs controls

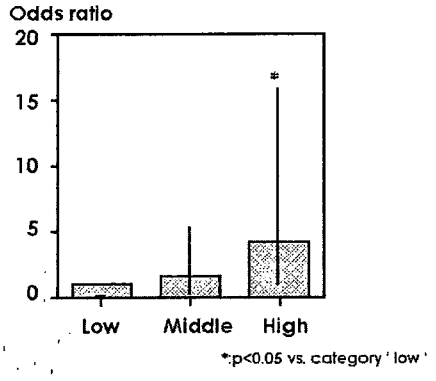

Fig. 1. Association of knee osteoarthritis with heaviest weight in the past. *Low*, lowest 3rd of the heaviest weight category, <61.0 kg; *Middle*, middle 3rd, ≥61.0 kg, <72.0 kg; *High*, highest 3rd, ≥72.0 kg. *Bar* represents 95% confidence interval

Table 2. Occupations reported as initial and principal jobs in men

	Initial occupation				Principal occupation			
	Cases	%	Controls	%	Cases	%	Controls	%
Total	37	100	37	100	37	100	37	100
Factory/construction workers	18	48.6	14	37.8	22	59.5	16	43.2
Agricultural/fishery workers	10	27.0	6	16.2	7	18.9	4	10.8
Clerical workers/technical experts	4	10.8	6	16.2	2	5.4	9	24.3
Shop assistants and managers	2	5.4	9	24.3	2	5.4	6	16.2
Clinical workers	2	5.4	0	0.0	1	2.7	0	0.0
Housekeepers	0	0.0	0	0.0	0	0.0	0	0.0
Hairdressers	0	0.0	0	0.0	0	0.0	0	0.0
Dressmakers	0	0.0	0	0.0	0	0.0	0	0.0
Teachers	0	0.0	0	0.0	2	5.4	0	0.0
Others (soldier, taxi driver, etc.)	1	2.7	2	5.4	1	2.7	2	5.4
No work, no answer	0	0.0	0	0.0	0	0.0	0	0.0

Table 3. Crude and adjusted odds ratios with risk factors for knee osteoarthritis in men

Men	Risk factors	Crude odds ratio (95% CI)	Adjusted odds ratio (95% CI)
Heaviest reported weight[a]	Middle vs Low	1.60 (0.50–5.08)	1.25 (0.29–5.35)
	High vs Low	4.22 (1.13–15.8)*	6.01 (1.18–30.5)*
Past injury of either knee	Yes vs No	2.50 (0.78–7.97)	6.25 (1.13–34.5)*
Occupational factors	Physical work[b] as principal occupation (vs Others)	2.80 (1.01–7.77)*	6.20 (1.40–27.5)*

Adjusted odds ratio refers to values after mutual adjustment for other potential risk estimates
95% CI, 95% confidence interval
[a]Lowest 3rd, <61.0 kg; middle 3rd, ≥61.0 kg, <72.0 kg; highest 3rd, ≥72.0 kg in men
[b]Physical work meaning factory, construction, agriculture or fishery work
* $P < 0.05$

Table 4. Crude and adjusted odds ratios with risk factors for knee osteoarthritis in women (cited from ref. 10)

Women	Risk factors	Crude odds ratio (95% CI)	Adjusted odds ratio (95% CI)
Heaviest reported weight[a]	Middle (vs Low)	1.68 (0.79–3.84)	3.33 (0.95–11.7)
	High (vs Low)	3.10 (1.26–7.98)*	3.92 (1.03–14.8)*
Past injury of either knee	Yes vs No	5.00 (2.44–10.2)*	7.51 (2.40–23.5)**
Transportation	Cycling almost every day for ≥12 months (vs Less)	1.88 (1.02–3.94)*	1.67 (0.61–4.57)
Occupational factors	Physical work[b] as initial occupation (vs Others)	2.54 (1.34–4.82)**	2.08 (0.88–5.61)
	Sitting ≥2 h/day at initial job (vs Less)	0.43 (0.23–0.78)**	0.44 (0.47–1.10)
	No. of jobs (1 job)	1.24 (1.02–1.50)*	0.91 (0.66–1.25)
	Total working period (1 year)	1.05 (1.03–1.07)***	1.05 (1.01–1.08)**

Adjusted odds ratio refers to values after mutual adjustment for other potential risk estimates
95% CI, 95% confidence interval
[a]Lowest 3rd, <55.0 kg; middle 3rd, ≥55.0 kg, <62.0 kg; highest 3rd, ≥62.0 kg in women
[b]Physical work meaning factory, construction, agriculture or fishery work
* $P < 0.05$; ** $P < 0.01$; *** $P < 0.001$

significantly between cases and controls. Physical work (factory/construction or agriculture/fishery) at the principal job was significantly more common among cases than controls (OR 2.80, 95% CI 1.01–7.77 for yes vs no). Mean age at commencement of the first job was 16.3 years (SD 3.8 years) compared to 16.6 years (SD 4.1 years) for controls, indicating no significant difference between cases and controls. Occupational activities including standing, climbing stairs, kneeling, squatting, driving, walking, sitting, and heavy lifting were not associated with increased risk of knee OA in men.

Table 3 shows ORs determined using conditional logistic regression analysis mutually adjusted for potential risk factors. Various risk factors were entered into the conditional logistic model, comprising: heaviest reported weight; previous knee injury; and physical work at the principal occupation in men. Heaviest reported weight in the past (OR 6.01, 95% CI 1.18–30.5, $P < 0.05$), past injury of the knee (OR 6.25, 95% CI 1.13–34.5, $P < 0.05$), and physical work at the principal occupation (OR 6.20, 95% CI 1.40–27.5, $P < 0.05$) represented independent factors associated with knee OA after controlling for other risk factors (Table 3).

Discussion

The results of the present case-control study indicate that heavy weight in the past and previous knee injury are associated with knee OA in men. Also in men, the proportion engaged in physical work (factory, construction, agriculture, or fishery work) was significantly higher among cases than controls. These risk factors for male knee OA are similar to those seen for female OA knees. Although we have already reported the results elsewhere,[10] we briefly compared results for men and women. Table 4 shows ORs in women determined using conditional logistic regression analysis mutually adjusted for potential risk factors. Various risk factors were entered into the conditional logistic model, comprising: heaviest reported weight in the past; previous knee injury; regular bicycle use; physical work in initial occupation; sedentary work in initial occupation; number of jobs; and total working period, summarizing all years of all jobs that subjects worked. Heaviest reported weight in the past, past injury of the knee, and total working period in women represented independent factors associated with knee OA after controlling for other risk factors. The results of the present case-control study indicate that heavy weight in the past and previous knee injury are associated with knee OA in both men and women.

Several limitations apply to the present study. Firstly, this investigation was based on a relatively small number of male cases and controls. Before the start of the research, we had calculated the sample size. We accumulated 155 pairs of cases and controls based on assumed values of a 0.05 level of significance, 80% statistical power, 2.0 risk ratio, and the 30% prevalence of cases. As a result, we succeeded in identifying 160 cases (40 men, 120 women) >45 years old

Table 5. Comparison of risk factors for hip and knee osteoarthritis (OA) in Britain and Japan (combined results for men and women)

	Risk factors	Britain	Japan
Hip OA	Obesity	Yes	No
	Past joint disturbance	Yes	No
	Occupational factors	Yes (lifting)	Yes (lifting)
Knee OA	Obesity	Yes	Yes
	Past joint disturbance	Yes	Yes
	Occupational factors	Yes (kneeling/squatting)	Yes (physical work, working period)

who fulfilled the entry criteria for the study. Of the eligible cases, 138 (86.3%; 37 men, 101 women) agreed to participate. However, the lack of gender balance for cases resulted in a small number of male subjects, which might reduce statistical power, and thus might not have detected other risk factors among lifestyle variables. This could be due to the use of identical case definitions for subject selection as the case-control hip OA and British studies. Cases were defined as those suffering knee pain and walking difficulties, who were first diagnosed by an orthopedic surgeon as displaying a tibiofemoral joint with a radiographic grade of ≥3 on the Kellgren and Lawrence scale. Our previous comparative study of OA in the lumbar spine indicated that OA in the general population tends to display lower prevalence and severity in Japan than in Britain.[14] In addition, the small number of male cases reflects gender differences in prevalence of knee OA in Japan. As a second limitation in the present study, the response rate for controls (52.8%) was lower than that for cases (92.0%). The present results may therefore be subject to some degree of overestimation.

Obesity has previously been shown to display strong associations with risk of knee OA,[2–8] and epidemiological studies performed in Japan have confirmed associations between obesity and knee OA.[15,16] In the present study, a history of heavy weight was shown to exert significant influences on risk of knee OA among men, resembling the results of women,[10] and consistent with previous studies. These findings indicate that the influence of heavy weight on knee OA is consistent across gender in both Japanese and Western populations.

The involvement of other joints is believed to play a role in increased risk of OA. In the British study paralleling the present study, presence of Heberden's node and previous knee injury were both strongly and independently associated with knee OA.[11,12] Although the present study did not seek information regarding the presence of Heberden's node, information was obtained about past history of the involvement of other joints and areas, as diagnosed by a medical doctor, indicating an independent association between previous knee injury and knee OA. In particular, site of knee OA was basically in accordance with the injured site among cases with previous knee injured (right side 91.7%, left side 100%). These findings were again consistent among men and women across Japanese and Western populations.

Mechanical stress represents another factor in the pathogenesis of OA at any joint site. In the present study, although occupational activities of standing, climbing stairs, kneeling, squatting, driving, walking, and heavy lifting were not associated with increased risk of knee OA in men, physical work at the principal occupation raised the risk of knee OA. Physical work represented by factory, construction, agricultural, or fishery work for long periods involved mechanical stress on the knee joints. The previous report utilized conditional logistic regression analysis without physical work, and identified sedentary work as a preventive factor in women.[10] These occupational activities influencing the risk of knee OA suggest that excess stress at the joint raises the risk, while reduced load on the joint decreases risk.

The present case-control study of knee OA paralleled our previous study of hip OA,[9] and was identical in format to some British studies.[17,18] Table 5 summarizes the results of studies using the same methods, indicating differences in risk factors between hip OA and knee OA, and between populations in Britain and Japan. Occupational factors clearly influence the development of both of hip and knee OA in Japan, as in Britain, although differences exist in specific activities exerting influence. Moreover, previous joint injury represented a risk factor for knee OA in Japan, as in the British studies. Conversely, obesity did not represent an independent risk factor for hip OA in Japan, but was a risk factor for both hip and knee OA in the British studies. This may be because local mechanical factors such as acetabular dysplasia might exert stronger influences on hip OA in Japan than other general mechanical factors such as adiposity. However, these results suggest that the pathogenesis of knee OA is similar in Japan and Western countries. Further studies of OA in other sites are required to characterize the risk profile in Japan.

Acknowledgments This research was supported by Grants-in-Aid for Scientific Research A11770200 from the Ministry of Education, Science, Sports and Culture in Japan, the Japan Society for the Promotion of Science, Research Society for Metabolic Bone Diseases, Japan, and the Arthritis Research Campaign, UK. We wish to acknowledge the generosity of surgeons and internists in Saiseikai Wakayama Hospital, Wakayama; Hori Hospital, Sennan; Nishioka Orthopaedic Hospital, Arita; Ryujin Clinic, Wakayama; Tamai Orthopaedic Hospital, Hannan; and Yamamoto Clinic, Shimotsu, Japan; and of Mrs. Sumiko Suzuri for help in locating participants for interviewing. The results of

this study were presented in 2001 at the British Society for Rheumatology XVIIIth Annual General Meeting.

References

1. Murray CJL, Lopez AD. The global burden of disease. Geneva: World Health Organization; 1997.
2. Anderson JJ, Felson DT. Factors associated with osteoarthritis of the knee and the first national health and nutrition examination survey (NHANES-I): evidence for an association with overweight, race and physical demands for work. Am J Epidemiol 1988;128: 179–89.
3. Felson DT. The epidemiology of knee osteoarthritis: results from the Framingham Osteoarthritis Study. Semin Arthritis Rheum 1990;20 Suppl 1:42–50.
4. Spector TD. The fat on the joint: osteoarthritis and obesity. J Rheumatol 1990;17:283–4.
5. Felson DT, Zhang Y, Anthony JM, Naimark A, Anderson JJ. Weight loss reduces the risk for symptomatic knee osteoarthritis in women. Ann Intern Med 1992;116:535–9.
6. Hochenburg MC, Lethbridge-Cejku M, Scott WW, Reichle R, Plato CC, Tobin JD. The association of body weight, body fatness and body fat distribution with osteoarthritis of the knee: data from the Baltimore longitudinal study of aging. J Rheumatol 1995;22: 488–93.
7. Hart DJ, Doyle DV, Spector TD. Incidence and risk factors for radiographic knee osteoarthritis in middle-aged women: the Chingford Study. Arthritis Rheum 1999;42:17–24.
8. Cooper C, Snow S, McAlindon RW, Kellingray S, Stuart B, Coggon D, et al. Risk factors for the incidence and progression of radiographic knee osteoarthritis. Arthritis Rheum 2000;43:995–1000.
9. Yoshimura N, Sasaki S, Iwasaki K, Danjoh S, Kinoshita H, Yasuda T, et al. Occupational lifting is associated with hip osteoarthritis: a Japanese case-control study. J Rheumatol 2000;27: 434–40.
10. Yoshimura N, Nishioka S, Kinoshita H, Hori N, Nishioka T, Ryujin M, et al. Risk factors for knee osteoarthritis in Japanese women: heavy weight, past joint injuries and occupational activities. J Rheumatol 2004;31:157–62.
11. Cooper C, McAlindon T, Coggon D, Egger P, Dieppe P. Occupational activity and osteoarthritis of the knee. Ann Rheum Dis 1994;53:90–3.
12. Coggon D, Croft P, Kellingray S, Barrett D, McLaren M, Cooper C. Occupational physical activities and osteoarthritis of the knee. Arthritis Rheum 2000;43:1443–9.
13. Kellgren JH, Lawrence JS. Radiological assessment of osteoarthritis. Ann Rheum Dis 1957;16:494–502.
14. Yoshimura N, Dennison E, Wilman C, Hashimoto T, Cooper C. Epidemiology of chronic disc degeneration and osteoarthritis of the lumbar spine in Britain and Japan: a comparative study. J Rheumatol 2000;27:429–33.
15. Tamaki M, Koga Y. Osteoarthritis of the knee joint: a field study (in Japanese). Nippon Seikeigeka Gakkai Zasshi (J Jpn Orthop Assoc) 1994;68:737–50.
16. Suematsu N, Onozawa T, Suzuki S, Takemitsu Y, Niinuma R. Epidemiologic study of osteoarthritis of the knee in agricultural and forestry workers (in Japanese). Seikei Saigai Geka (Orthop Surg Traumatol) 1986;29:343–6.
17. Cooper C, Inskip H, Croft P, Campbell L, Smith G, McLaren M, et al. Individual risk factors for hip osteoarthritis; obesity, hip injury, and physical activity. Am J Epidemiol 1998;147:516–22.
18. Coggon D, Kellingray S, Inskip H, Croft P, Campbell L, Cooper C. Osteoarthritis of the hip and occupational lifting. Am J Epidemiol 1998;147:523–8.

Cell Transplantation, Vol. 14, pp. 683–693, 2005
Printed in the USA.

0963-6897/05 $20.00 + .00
E-ISSN 1555-3892
www.cognizantcommunication.com

Synergistic Effects of FGF-2 With Insulin or IGF-I on the Proliferation of Human Auricular Chondrocytes

Tsuguharu Takahashi,*† Toru Ogasawara,*‡ Junji Kishimoto,§ Guangyao Liu,*¶ Hirotaka Asato,# Takashi Nakatsuka,** Eijyu Uchinuma,†† Kozo Nakamura,§ Hiroshi Kawaguchi,§ Tsuyoshi Takato,†‡ and Kazuto Hoshi*†

*Department of MENICON Cartilage & Bone Regeneration, Graduate School of Medicine and Faculty of Medicine, The University of Tokyo, Hongo 7-3-1, Bunkyo-Ku, Tokyo 113-0033, Japan
†Division of Tissue Engineering, Graduate School of Medicine and Faculty of Medicine, The University of Tokyo, Hongo 7-3-1, Bunkyo-Ku, Tokyo 113-0033, Japan
‡Department of Oral & Maxillofacial Surgery, Graduate School of Medicine and Faculty of Medicine, The University of Tokyo, Hongo 7-3-1, Bunkyo-Ku, Tokyo 113-0033, Japan
§Department of Clinical Bioinformatics, Graduate School of Medicine and Faculty of Medicine, The University of Tokyo, Hongo 7-3-1, Bunkyo-Ku, Tokyo 113-0033, Japan
¶Department of Orthopaedics Surgery, Graduate School of Medicine and Faculty of Medicine, The University of Tokyo, Hongo 7-3-1, Bunkyo-Ku, Tokyo 113-0033, Japan
#Department of Plastic & Reconstructive Surgery, Graduate School of Medicine and Faculty of Medicine, The University of Tokyo, Hongo 7-3-1, Bunkyo-Ku, Tokyo 113-0033, Japan
**Department of Plastic & Reconstructive Surgery, Saitama Medical School, Kerohongo 38, keroyama-cho, Iruma, Saitama 350-0495, Japan
††Department of Plastic & Reconstructive Surgery, Kitasato University, Kitasato 1-15-1, Sagamihara, Kanagawa 228-8555, Japan

Chondrocyte preparation with the safety and efficiency is the first step in cartilage regenerative medicine. To prepare a chondrocyte proliferation medium that does not contain fetal bovine serum (FBS) and that provides more than a 1000-fold increase in cell numbers within approximately 1 month, we attempted to use the medium containing 5% human serum (HS), but it exerted no more than twofold increase in 2 weeks. To compensate for the limited proliferation ability in HS, we investigated the combinational effects of 12 factors [i.e., fibroblast growth factor(FGF)-2, insulin-like growth factor(IGF)-I, insulin, bone morphogenetic protein-2, parathyroid hormone, growth hormone, dexamethasone, 1α25-dihydroxy vitamin D_3, L-3,3′,5′-triodothyronine, interleukine-1 receptor antagonist, 17β-estradiol, and testosterone] on the proliferation of human auricular chondrocytes by analysis of variance in fractional factorial design. As a result, FGF-2, dexamethasone, insulin, and IGF-I possessed promotional effects on proliferation, while the combination of FGF-2 with insulin or IGF-I synergistically enhanced the proliferation. Actually, the chondrocytes increased 7.5-fold in number in 2 weeks in a medium containing 5% HS with 10 ng/ml FGF-2 , while the cell number synergistically gained a 10–12-fold increase with 5 μg/ml insulin or 100 ng/ml IGF-I in the same period. The proliferation effects were more enhanced at a concentration of 100 ng/ml for FGF-2, and especially for the combination of 100 ng/ml FGF-2 and 5 μg/ml insulin (approximately 16-fold within 2 weeks). In the long-term culture with repeated passaging, this combination provided more than 10,000-fold within 8 weeks (i.e., passage 4). Thus, we concluded that such a combination of FGF-2 with insulin or IGF-I may be useful for promotion of auricular chondrocyte proliferation in a clinical application for cartilage regeneration.

Key words: Chondrocyte; Proliferation; Regenerative medicine; Medium; Soluble factor; Fractional factorial design

INTRODUCTION

Tissue engineering is a challenging technology in which the tissues or the cells are cultured in the laboratory and are used for replacement or support of the function of defective or injured body parts. This new approach is anticipated to overcome the difficulties or problems in the present clinical treatment. Recently, the studies on tissue engineering have endeavored to grow every type of human tissue: liver, bone, muscle, carti-

Address correspondence to Kazuto Hoshi, M.D., Ph.D., Department of Fujisoft ABC Cartilage & Bone Regeneration, Graduate School of Medicine, The University of Tokyo, Hongo 7-3-1, Bunkyo, Tokyo 113-8655, Japan. Tel: 81-3-3815-5411, ext. 37386; Fax: 81-3-5800-9891; E-mail: pochitky@umin.ac.jp

lage, blood vessels, heart muscles, nerves, pancreatic islets, and more. Among them, cartilage regenerative medicine has progressed well. Tissue-engineered cartilage has already been available for clinical use in the treatment of patients with joint defects (5,22,23) or for the correction of vesicoureteral reflux (6).

However, to broaden the indication range of cartilage regenerative medicine (e.g., to microtia, which is a congenital anomaly of the ear, cleft lip and palate, or osteoarthritis), some improvement would be necessary. One of issues to be improved is cell preparation with safety and efficiency. We should obtain a sufficient cell number from a small volume of specimen within a limited period, for clinical use. In a previous report on autologous chondrocyte transplantation for joint defects, a culture medium with 10% autologous human serum provided approximately 5×10^6 cells within 3 weeks, corresponding to 0.3–0.4 ml of regenerative cartilage material (23). However, because the volume of the regenerative cartilage needed in the treatment of microtia or end-stage osteoarthritis of knees may be some tens of milliliters, more than a 100-fold increase in cell numbers would need to be prepared for such cases, compared with that in an autologous transplantation.

To improve the efficiency of cell preparation, many researchers have attempted to use growth factors with fetal bovine serum (FBS). Quatela and coworkers examined the proliferation of human auricular chondrocytes in DMEM containing 5% FBS with 10 ng/ml fibroblast growth factor (FGF)-2 and 3 ng/ml transforming growth factor (TGF)-β, which exerted a maximal synergistic effect on thymidine uptake (25).

Although FBS contains various factors that can increase chondrocyte proliferation (7,10), the use of FBS may be restricted for clinical application because it includes the risk for transmission of viral and other pathogens. In addition, problems of possible immune reaction against bovine protein in the serum should be considered when the regenerated tissues cultured in the FBS-contained medium are transplanted into humans. The previous studies had shown immune response by antibody detection against bovine serum proteins in burn patients receiving keratinocyte grafts cultured from FBS (12,19).

Under clinical conditions, we may use human serum (HS) obtained from the patients by autologous blood transfusion, which would help the proliferation of their own cells. With HS, we statistically examined the additional effectiveness of soluble factors with regard to their synergy in chondrocytes obtained from the patients. For this experiment, we chose 12 kinds of soluble factors, all of which possess some effect on chondrocyte proliferation or differentiation and are clinically available because their safety has already been secured. Using the statistical method that is termed "analysis of variance by fractional factorial design" (8), the effects of the individual factors and the synergy of combinations were evaluated. This statistical method is useful when the number of potential factors is large, because it can minimize the total numbers of runs required. According to this method, we selected highly effective combinations of soluble factors for proliferation of human auricular chondrocytes, which might be immediately applied in the clinical field.

MATERIALS AND METHODS

Growth Factors and Reagents

Dulbecco's modified Eagle's medium (DMEM), DMEM nutrient mixture F-12 HAM (DMEM/F12), penicillin-streptomycin solution, trypsin-EDTA solution, fetal bovine serum (FBS), and human serum (HS, lot# 043K0500, 043K0501, and 043K0502) were purchased from Sigma Chemical Co. (St. Louis, MO, USA). Dexamethasone (Dex), 1α25-dihydroxy vitamin D_3 (vitD), L-3,3′,5′-triiodothyronine (T3), and 17β-estradiol (E_2) were from EMD Bioscience (San Diego, CA, USA). Collagenase from *Clostridium histolyticum* and ISOGEN were from Wako Pure Chemical Industries, Ltd. (Osaka, Japan). Other reagents were: atelocollagen (Kawaken Fine Chemicals Co., Ltd., Tokyo, Japan), bullet kit chondrocyte growth medium (CGM, Cambrex Bioscience Walkersville, Inc., Walkersville, MD, USA), FGF-2 (kindly provided by Kaken Pharmaceutical Corporation, Ltd., Tokyo, Japan), recombinant human insulin-like growth factor-I (IGF-I, former Genzyme-Techne, Minneapolis, MN), insulin (MP Biomedicals Inc., Irvine, CA, USA), recombinant human bone morphogenetic protein-2 (BMP-2, kindly provided by Yamanouchi Pharmaceutical Co., Ltd., Tokyo, Japan), human parathyroid hormone [PTH (1–34), Anaspec, Inc., San Jose, CA], human growth hormone (GH, Biogenesis, Ltd., Poole, UK), recombinant human interleukin-1 receptor antagonist (IL-1 RA, Strathmann Biotech GmbH, Hamburg, Germany), and testosterone (Ultrafine Chemicals, Manchester, UK).

Cell Isolation

All procedures of the present experiments were approved by the ethic committee of the University of Tokyo Hospital (ethic permission #622). Remnant auricular cartilage and surgical debris of the costal cartilage were obtained from five children (age range 10–15 years) who underwent microtia surgery at the University of Tokyo Hospital, with informed consent. The perichondrium was separated from the auricular cartilage under sterile conditions, while that of the costal cartilage had been already removed during the operation. The isolated cartilage was minced into 1-mm^3 pieces and digested with 0.15% collagenase in DMEM containing penicillin and streptomycin at 37°C for 24 h. The digested suspen-

sion was filtered using a sterile 100-μm nylon cell strainer (BD Falcon, Bedford, MA, USA) and centrifuged at 430 × *g* for 5 min. The resulting pellet of cells was washed twice with DMEM containing the antibiotics and then resuspended in the medium. The number of cells was calculated using a hemocytometer, and the viability of the cells was determined using trypan blue vital dye.

Chondrocyte Culture and Evaluation of Proliferation

Chondrocytes were suspended in 0.24% atelocollagen solution (pH 7). The mixture was placed in each well of a six-well plate at 2 ml, or a 96-well plate for 0.1 ml, at a density of 2×10^4 cells/ml. The atelocollagen formed a gel in 1-h incubation at 37°C, embedding the cells in a 3D condition. The commercial medium, CGM containing 5% FBS with an undisclosed concentration of FGF-2, IGF-I, and insulin, or the medium containing DMEM/F-12 with or without serum and/or soluble factors was gently poured on the gel at a volume of 2 ml or 0.1 ml, respectively, in a 37°C/5% CO_2 incubator. Throughout the experiment, the medium was changed three times per week. To release the cells, the gel was incubated in 0.3% collagenase at 37°C for 2 h.

To evaluate the cell proliferation by cell count, the auricular chondrocytes (cultured in CGM, passage 4) from the five patients were individually incubated in five wells of a six-well plate for each medium. After a 2-week incubation, the cell numbers were counted by a hematocytometer, while the viability of cells was checked by trypan blue staining. For the long-term culture with repeated passaging of the auricular or costal chondrocytes, we cultured the cells in three wells of six-well plates with the CGM or the DMEM/F-12 with 5% HS and soluble factors. Passage was performed every week or every other week, while the mean cell numbers in the three wells were counted during every passage.

To evaluate the samples on the 96-well plates, we used a colorimetric assay for cell proliferation, Cell Proliferation Kit II (Roche Molecular Biochemicals, Mannheim, Germany). Briefly, after the release of chondrocytes from the gel in each well of the 96-well plates, the cells were centrifuged for 5 min at 430 × *g* and separated from the supernatant, which was then removed. The labeling mixture was then added to the cells, which were incubated for 4 h in a 37°C/5% CO_2 incubator. The spectrophotometric absorbance of the samples using a microtiter plate reader was measured at a wavelength of 450 nm. The reference wavelength was 650 nm.

Fractional Factorial Design

Twelve factors (i.e., FGF-2, IGF-I, insulin, BMP-2, PTH, GH, Dex, vitD, T3, IL-1RA, E_2, and testosterone) were examined for their combinational effects on proliferation. The doses of each factor were used from previous papers or were determined as their modifications due to our own preliminary data and/or economical reasons (Table 1). With the usual factorial design, $2^{12} = 4096$ treatment combinations would be needed, but this is practically impossible. We adopted fractional factorial design (8) to reduce the experimental units to a practical number of 256 combinations. This design retains good statistical properties and has found its greatest use in industrial research. We used the software JMP-5.1.1J (SAS Institute, Inc., Cary, NC, USA) to generate the 256 kinds of randomized combinations in which those 12 factors independently appeared on the incidence of 50% (Table 2). We then made the same number of media containing DMEM/F-12 with those combinations of factors and 5% HS. Three kinds of auricular chondrocytes obtained from different patients were incubated in each well of 96-well plates with those media for 2 weeks. The effects of each medium on proliferation were examined in the colorimetric assay for cell proliferation. Values for three kinds of auricular chondrocytes in each media were processed by analysis of variance using the software JMP, providing an *F*-value, meaning the effects of the individual factors or the interaction terms of two factors, as well as a parameter estimate indicating expected changes produced by one factor or two. Total effect of two factors on proliferation was compared with each other, as the sum of parameter estimates of two main effects and interaction.

Total RNA Extraction and Real-Time PCR

The chondrocytes were released from the atelocollagen gel by a 30-min incubation in 0.3% collagenase. The total RNA was isolated from the chondrocytes with ISOGEN following the supplier's protocol. Complementary DNA (cDNA) was synthesized from 1 μg of total

Table 1. Twelve Soluble Factors Affecting Chondrocyte Proliferation and Differentiation

Soluble Factors	Doses	References
FGF-2	10 ng/ml	13
IGF-I	100 ng/ml	30
Insulin	5 μg/ml	14
BMP-2	200 ng/ml	27
PTH	5×10^{-8} M	32
GH	100 ng/ml	20
Dex	10^{-7} M	21
VitD	10^{-7} M	11
T3	10^{-7} M	17
IL-1 RA	20 ng/ml	31
E_2	10^{-7} M	26
Testosterone	10^{-6} M	18